NATIONAL ADVISORY COMMITTEE FOR AERONAUTICS

TECHNICAL NOTE 3296

SEPARATION, STABILITY, AND OTHER PROPERTIES OF COMPRESSIBLE LAMINAR BOUNDARY LAYER WITH PRESSURE GRADIENT AND HEAT TRANSFER

By Morris Morduchow and Richard G. Grape

Polytechnic Institute of Brooklyn

Washington

May 1955

R

NATIONAL ADVISORY COMMITTEE FOR AERONAUTI

TECHNICAL NOTE 3296

SEPARATION, STABILITY, AND OTHER PROPERTIES OF COMPRESSIBLE LAMINAR BOUNDARY LAYER WITH PRESSURE GRADIENT AND HEAT TRANSFER

By Morris Morduchow and Richard G. Grape

SUMMARY

A theoretical study is made of the effect of pressure gradient, wall temperature, and Mach number on laminar boundary-layer characteristics and, in particular, on the skin-friction and heat-transfer coefficients, on the separation point in an adverse pressure gradient, on the wall temperature required for complete stabilization of the laminar boundary layer, and on the minimum critical Reynolds number for laminar stability. The Prandtl number is assumed to be unity and the coefficient of viscosity is assumed to be proportional to the temperature, with a factor arising from the Sutherland relation. A simple and accurate method of locating the separation point in a compressible flow with heat transfer is developed. Numerical examples to illustrate the results in detail are given throughout.

INTRODUCTION

The purpose of the present investigation is to determine theoretically the nature of the laminar boundary layer in compressible flow with heat transfer and pressure gradient. In particular, the effect of pressure gradient (favorable and adverse), wall temperature, and Mach number on the boundary-layer characteristics are investigated. Such an investigation has already been made in reference 1 on the basis of fourth-degree velocity and stagnation-enthalpy profiles, in conjunction with two different boundary-layer thicknesses (a dynamical and a thermal boundary-layer thickness). In contrast with the present study, the effect of normal fluid injection at the wall was included in reference 1, but the stability of the boundary layer was not investigated therein. The present investigation is based on the more accurate method of calculating boundary-layer properties as developed in reference 2, where sixth-degree velocity and seventh-degree stagnation-enthalpy profiles are applied in conjunction with a single boundary-layer thickness, with the thermal boundary-layer thickness replaced by an additional parameter b_1 in the stagnation-enthalpy profile.

In the first section of this study, skin-friction and heat-transfer characteristics are investigated, especially with respect to the effect of wall temperature, pressure gradient, and Mach number. The analysis is carried out first in general terms and then illustrated by a numerical example for the supersonic flow over a thin airfoil, for which the pressure gradient is everywhere favorable (negative). In the next section, a simple and ordinarily sufficiently accurate method of calculating the separation point in an adverse pressure gradient in subsonic or supersonic flow[1] over a wall at a given uniform temperature is developed. The method, based on the special use of a seventh-degree profile to satisfy an additional boundary condition at the separation point (first suggested in ref. 3), is essentially an extension of the method developed for zero heat transfer in reference 4, where a numerical example indicated excellent agreement with exact results. With this method, the effect of wall temperature and Mach number on the separation point is investigated. The results are then illustrated by a numerical example for flow with a linearly decreasing velocity outside of the boundary layer. A second example treats the conditions (involving the wall temperature) under which laminar separation will take place immediately behind a stagnation flow abruptly followed by an adverse pressure gradient.

In the final section, the stability of the laminar boundary layer over a thin biconvex airfoil in supersonic flow is investigated. For this purpose, the wall temperature required for complete stabilization of the flow (infinite minimum critical Reynolds number) is calculated for several Mach numbers at different stations along the airfoil. In addition, the minimum critical Reynolds number is determined at a given station for various wall temperatures and Mach numbers. Comparison is made with results for flow over a flat plate in order to demonstrate the effect of a pressure gradient, in addition to that of wall temperature, on the stability characteristics. The stability calculations here are based on the well-known two-dimensional criteria developed by Lees and Lin (refs. 5 and 6) for compressible flow. Since the validity of these criteria appears at present to be in doubt for high Mach numbers (e.g., ref. 7), the present calculations have been restricted to Mach numbers not above 3. The present results on stability characteristics in compressible flow with heat transfer and pressure gradient may, in a sense, be considered as an extension of the results already obtained for flow over a flat plate (zero pressure gradient) with heat transfer (refs. 8 to 11) and for flow with a pressure gradient but without heat transfer at the wall (refs. 12 and 4).

The analysis in the present investigation is based on the assumption of a uniform wall temperature, a Prandtl number of unity, and a linear

---

[1]Shock-wave interaction with the boundary layer, however, is not considered.

temperature-viscosity relation (as in ref. 1). As in reference 2, however, a factor C (first suggested and applied in ref. 13) has been introduced in the temperature-viscosity relation to account, at least at the wall, for the Sutherland viscosity law. This factor, as will be seen, has an influence on the skin-friction and heat-transfer coefficients, although not on the separation point. One simple, but very approximate, means of correcting the Nusselt numbers to be obtained here in cases of a Prandtl number different from unity would be to multiply the Nusselt numbers for unit Prandtl number by a power of the actual Prandtl number, this power being roughly equal to 1/3 (cf., e.g. refs. 14 and 15).

This investigation was conducted at the Polytechnic Institute of Brooklyn Aeronautical Laboratories under the sponsorship and with the financial assistance of the National Advisory Committee for Aeronautics. The authors hereby express their thanks to Professors P. A. Libby and M. Bloom for their helpful discussions and to Mr. Richard P. Shaw for his aid in the calculations.

SYMBOLS

a_2	coefficient of τ^2 in velocity profile; see also equation (6)
$\bar{a}_2$	constant average value of a_2
a_{2s}	value of a_2 at separation point
b_1	coefficient of τ in stagnation-enthalpy profile
$\bar{b}_1$	constant average value of b_1
C	factor in viscosity-temperature relation (eqs. (1) and (2))
C_{f_l}	local skin-friction coefficient
c_p	specific heat at constant pressure
c_v	specific heat at constant volume
$\bar{F}_1$	constant, given by equation (8)
$\bar{F}_{1s}$	constant used instead of $\bar{F}_1$ in determining separation point; see equation (24)

G_1 ratio of stagnation enthalpy at wall to stagnation enthalpy at outer edge of boundary layer, H_o/H_1; for a Prandtl number of 1, G_1 is ratio of actual wall temperature T_o to equilibrium wall temperature T_e for zero heat transfer (see also eq. (13))

H stagnation enthalpy, defined as quantity $(u^2/2) + c_pT$

K_1, K_2 constants (see eqs. (28) and (29))

k thermal conductivity

k_1, k_2 coefficients in velocity distribution over thin airfoil (eqs. (17))

L characteristic length; chord length for airfoil of figure 1

M Mach number

Nu Nusselt number

R_∞ Reynolds number, $u_\infty L/\nu_\infty$

R_b Reynolds number, $u_b L/\nu_b$

$R_{b,cr}$ minimum critical Reynolds number, based on conditions at point b immediately behind shock wave at leading edge of airfoil in figure 1, $(u_b L/\nu_b)_{cr}$

$R_{\infty,cr}$ minimum critical Reynolds number, based on remote free-stream conditions in supersonic flow over thin airfoil of figure 1, $(u_\infty L/\nu_\infty)_{cr}$

r proportional to ratio of local skin friction to local Nusselt number (eq. (16))

S constant in Sutherland viscosity-temperature relation, 216° R for air

T absolute temperature

T_e equilibrium wall temperature for zero heat transfer; for a Prandtl number of unity, $T_e = T_\infty\left(1 + \frac{\gamma - 1}{2} M_\infty^2\right)$

t variable defined by equation (3)

u	velocity in x-direction
x,y	coordinates parallel and normal to surface, respectively
γ	ratio of specific heats, c_p/c_v, 1.4 for air
ρ	density
δ_t	boundary-layer thickness in xt-plane
η	geometric slope of thin airfoil profile
$\lambda = R_\infty(\delta_t/L)^2$	
μ	coefficient of viscosity
ν	kinematic viscosity
ξ	dimensionless distance along wall, x/L
$\xi' = x'/L$ (see fig. 1)	
τ	dimensionless variable, t/δ_t
φ_1	constant defined by equation (8)
φ_{1s}	constant used instead of φ_1 in determining separation point (see eq. (24))

Subscripts:

b	values at point outside of boundary layer immediately behind shock wave at leading edge of airfoil
cr	critical
fav	favorable pressure gradient
o	values at wall
s,sep	values at or used for determining separation point (see eqs. (23) and (21))
1	local values at outer edge of boundary layer

∞ values at suitable reference point outside of boundary layer; for airfoil in supersonic flow, values in undisturbed (remote) free stream

$'$ differentiation with respect to ξ

BASIC EQUATIONS

The basic equations for the calculation of the laminar-boundary-layer characteristics in compressible flow with an axial pressure gradient over a wall at a uniform wall temperature T_o have been developed in reference 2 with the assumptions that the Prandtl number is unity and that the coefficient of viscosity varies with temperature according to the relation

$$\mu/\mu_\infty = C(T/T_\infty) \tag{1}$$

where

$$C = (T_o/T_\infty)^{1/2}(T_\infty + S)/(T_o + S) \tag{2}$$

These equations will be repeated here for convenient reference. The variable t replaces the physical normal coordinate y according to the relation

$$y = \int_0^t (T/T_1)dt \tag{3}$$

The velocity and stagnation-enthalpy profiles are given, respectively, by

$$\frac{u}{u_1} = \left(2\tau - 5\tau^4 + 6\tau^5 - 2\tau^6\right) + \left(\frac{a_2}{5}\right)\left[-2\tau + 5\tau^2 - 10\tau^4 + 10\tau^5 - 3\tau^6 + \left(\frac{b_1}{6G_1}\right)\left(-\tau + 10\tau^3 - 20\tau^4 + 15\tau^5 - 4\tau^6\right)\right] \tag{4}$$

$$\frac{H}{H_1} = G_1 + \left(1 - G_1\right)\left(35\tau^4 - 84\tau^5 + 70\tau^6 - 20\tau^7\right) + b_1\left(\tau - 20\tau^4 + 45\tau^5 - 36\tau^6 + 10\tau^7\right) \tag{5}$$

where

$$a_2 = -(1/2C)(T_1/T_\infty)^{(2-\gamma)/(\gamma-1)}(u_1'/u_\infty)G_1\left(1 + \frac{\gamma - 1}{2} M_1^2\right)\lambda \tag{6}$$

and the dimensionless boundary-layer thickness $\lambda(\xi)$ in the xt-plane can be calculated from the equation

$$\lambda = \left(4/\bar{F}_1\right)C \frac{\int_0^\xi (u_1/u_\infty)^{\left(2/\bar{F}_1\right)\varphi_1 - 1} (T_1/T_\infty)^{\left[(2\gamma-1)/(\gamma-1)\right] - \left(\varphi_1/\bar{F}_1\right)} d\xi}{(u_1/u_\infty)^{\left(2/\bar{F}_1\right)\varphi_1} (T_1/T_\infty)^{\left[(\gamma+1)/(\gamma-1)\right] - \left(\varphi_1/\bar{F}_1\right)}} \tag{7}$$

Here $\bar{F}_1$ and φ_1 are constants defined as

$$\left.\begin{aligned} \bar{F}_1 &= 0.1093 + 0.00211\bar{a}_2 - 0.000622\overline{a_2^2} + 0.000412\left(\bar{b}_1\bar{a}_2/G_1\right) - \\ &\quad 0.0000095\left(\bar{b}_1\bar{a}_2/G_1\right)^2 - 0.000153\left(\bar{b}_1\overline{a_2^2}/G_1\right) \\ \varphi_1 &= 0.3G_1 + 0.00438 + 0.0232\bar{a}_2 - 0.00124\overline{a_2^2} + \\ &\quad \bar{b}_1\left[0.0905 + \left(\bar{a}_2/30G_1\right)\left(0.0838 - 0.00458\bar{a}_2\right)\right] \end{aligned}\right\} \tag{8}$$

where $\bar{a}_2$ and $\bar{b}_1$ denote constant average values of $a_2(\xi)$ and $b_1(\xi)$ over the entire flow.

Equation (7) is a solution of the ordinary differential equation

$$\left(\bar{F}_1/2\right)\lambda' + \lambda\left\{\bar{F}_1\left(\rho_1'/\rho_1\right) + \left(u_1'/u_1\right)\left[\varphi_1 + \frac{\gamma - 1}{2} M_1^2\left(\varphi_1 - \bar{F}_1\right)\right]\right\}$$
$$= 2C\left(\rho_\infty/\rho_1\right)\left(T_1/T_\infty\right)\left(u_\infty/u_1\right) \tag{9}$$

The coefficient $b_1(\xi)$ is a function of $a_2(\xi)$ and is to be calculated as the solution of a quadratic equation (eq. (68) of ref. 2) after $\lambda(\xi)$ and thence $a_2(\xi)$ have been determined. It will usually be found that an approximate value for b_1 is

$$b_1 \approx 2\left(1 - G_1\right) \tag{10}$$

(Eq. (10) is exactly valid for flow over a flat plate.) The temperature distribution T_1/T_∞ and the Mach number M_1 at the local outer edge of the boundary layer will be related to the velocity distribution $u_1/u_\infty(\xi)$ there according to the relations

$$T_1/T_\infty = 1 + \left[(\gamma - 1)/2\right]M_\infty^2\left[1 - \left(u_1/u_\infty\right)^2\right] \tag{11}$$

$$M_1^2 = \left(u_1/u_\infty\right)^2 M_\infty^2 \left(T_1/T_\infty\right)^{-1} \tag{12}$$

The wall-temperature ratio T_o/T_∞ is related to the parameter $G_1 = T_o/T_e$ by the relation

$$T_o/T_\infty = G_1\left(1 + \frac{(\gamma - 1)}{2} M_\infty^2\right) \tag{13}$$

The local skin-friction and heat-transfer (Nusselt number) coefficients follow, respectively, from the equations

$$C_{f_l} \equiv \frac{(\mu \partial u/\partial y)_o}{\frac{1}{2}\rho_\infty u_\infty^2} = 4\left[1 - \left(a_2/5\right) - \left(b_1 a_2/60 G_1\right)\right]\left(C/\sqrt{\lambda}\right)\left(T_1/T_\infty\right)\left(u_1/u_\infty\right)R_\infty^{-1/2} \tag{14}$$

$$Nu \equiv \frac{(k \partial T/\partial y)_o L}{k_\infty(T_o - T_e)} = \left(C/\sqrt{\lambda}\right)\left[b_1/\left(1 - G_1\right)\right]\left(T_1/T_\infty\right)R_\infty^{1/2} \tag{15}$$

SKIN-FRICTION AND HEAT-TRANSFER CHARACTERISTICS

From the foregoing equations, several general conclusions on the effect of wall temperature, pressure gradient, and Mach number on the skin-friction and Nusselt number can be derived.

General Implications

The effect of wall temperature on the skin-friction and heat-transfer coefficients arises essentially from two different sources: (a) The conditions of dynamic equilibrium, as defined mathematically by the basic differential equations and their solutions, and (b) the variation of the viscosity coefficient with temperature, as defined mathematically by the constant C.

With respect to (a), the effect of wall temperature will depend on the nature (positive or negative, i.e., adverse or favorable) of the pressure gradient. This follows from the fact that in the governing momentum ordinary differential equation (eq. (9)) the quantity G_1 appears primarily in a form multiplied by the velocity gradient u_1' in the flow outside of the boundary layer. This is also the case in the coefficient a_2 (eq. (6)). By bringing the u_1' term in equation (9) to the right side and observing the expression for φ_1 according to equation (8), it can be seen, in fact, that for $u_1' > 0$ (favorable pressure gradient) $(\lambda/C)'$, and hence (λ/C), will tend to be increased by a decrease in the wall-temperature parameter G_1.[2] This result, in conjunction with equations (14), (15), (6), and (10), indicates that, without the effect of C, lowering the wall temperature tends to diminish the local Nusselt number and, especially, the local skin friction in a favorable pressure gradient and to increase the Nusselt number and, especially, the skin friction in an adverse pressure gradient. This conclusion is in accord with that also derived in reference 1. It must be noted, however, that for a cooled wall, where $G_1 < 1$, the foregoing effect of wall temperature on a_2 due to a pressure gradient will ordinarily be greater than that on λ/C, since it will be found from the general solutions (7) and (8) that λ/C is then not very sensitive to changes in G_1.

From equations (14), (15), and (7) it follows that both the skin friction and Nusselt number will be proportional to $\sqrt{C}$. The effect of wall temperature arising from the viscosity coefficient and determined by the constant C is, contrary to the dynamical effect just discussed, independent of the pressure gradient. From equation (2) it follows that, if T_0/T_∞ is diminished, then C and hence C_{f_l} and Nu decrease when $T_0/T_\infty < S/T_\infty$ (or $T_0 < 216^\circ$ R), while C and hence C_{f_l} and Nu increase when $T_0/T_\infty > S/T_\infty$ (or $T_0 > 216^\circ$ R). The latter is expected to be the case in practice. Thus, depending on the nature of the pressure gradient and possibly on the magnitude of the wall temperature, the dynamical and viscosity effects of wall temperature may tend either to magnify or partly to cancel each other. More specifically, unless the wall is unusually cold, that is, unless $T_0 < S$, these effects will tend to oppose each other in a favorable pressure gradient and to magnify each other in an adverse pressure gradient.

---

[2]According to the equations developed here, this conclusion may not be quite valid in the immediate vicinity of a sharp leading edge where the pressure-gradient effect is relatively unimportant and the small effect of wall temperature on $\bar{F}_1$ may actually predominate. (Cf. table II in conjunction with the numerical example discussed subsequently.) In this vicinity, however, the dynamical effect of a uniform wall temperature will be found to be negligible.

It is significant to note that, since the velocity gradient u_1' appears in the equations (eqs. (6) and (9)) always multiplied by the wall-temperature ratio G_1, it can be inferred that a lowering of the wall temperature has a tendency to diminish the direct effect of a given pressure gradient, that is, the effect of u_1' as such, on the boundary-layer properties. A clear illustration of this will be seen subsequently in the analysis of laminar separation (cf. also ref. 1).[3] It must be observed, however, that the effect of a pressure gradient also appears indirectly, namely, in the variation of u_1/u_∞ and T_1/T_∞ with ξ. For Mach numbers above 1, in fact, the T_1/T_∞ terms in λ (eq. (7)) may become particularly important, so that in such a case the net effect of the pressure gradient may actually be increased by a lowering of the wall temperature. This will be clearly illustrated by the subsequent numerical example.

From equations (14) and (15) it follows that the ratio of local skin-friction coefficient to the local Nusselt number can be expressed as

$$r \equiv \left(\frac{C_{f_l}}{Nu}\right)\left(\frac{u_\infty}{u_1}\right)R_\infty = \frac{4(1 - G_1)}{b_1}\left[1 - \frac{a_2}{5}\left(1 + \frac{b_1}{12G_1}\right)\right] \tag{16}$$

Equation (16) is valid along the entire flow. For flow over a flat plate (zero pressure gradient: $u_1/u_\infty = 1$, $a_2 = 0$), equation (16) implies $r = 2$. For flow with a pressure gradient, however, this simple relation is seen to be no longer valid. Since, ordinarily, $4(1 - G_1)/b_1 \approx 2$, equations (16) and (6) imply $r > 2$ along the flow in a favorable pressure gradient ($u_1' > 0$) and $r < 2$ in an adverse pressure gradient ($u_1' < 0$). Thus the ratio r tends to be increased by a negative (favorable) pressure gradient and decreased by a positive (adverse) pressure gradient.[4] From equations (6) and (16) it is seen that, for a

---

[3]Further illustrations of this conclusion can be found in numerical examples of reference 16, which are based on a small-perturbation method.

[4]Equation (14) and hence equation (16) may be inaccurate at, and hence in the immediate vicinity of, the separation point in an adverse pressure gradient, since, according to the criterion of separation (eq. (20)) developed in the succeeding section "Location of Separation Point," C_{f_l} as given by equation (14) will not vanish exactly at the separation point. This is due to the use of sixth- instead of seventh-degree velocity profiles here. However, equations (14) and (16) should, for practical purposes, be adequate to yield the distribution of skin-friction along the flow. When the primary interest is in the location of the separation point, the method described in the section "Location of Separation Point" should be used.

given pressure gradient and Mach number, the lower the wall temperature the closer will r be to its value for flow without a pressure gradient. This illustrates the diminution of the direct effect of a pressure gradient by cooling of the wall.

From equation (7), as has already been noted, it will be found that in the presence of a pressure gradient λ/C may be appreciably affected by the Mach number because of the values of $T_1/T_\infty(\xi)$. Consequently it can be inferred, in view of equations (14) and (15), that a pressure gradient will in general tend to enhance the effect of Mach number on both the heat-transfer and skin-friction coefficients. Since the values of $T_1/T_\infty(\xi)$ will depend on the distribution of the velocity $u_1/u_\infty(\xi)$ along the flow (eq. (11)), this effect of Mach number will, in fact, depend on the nature of the pressure gradient. For a favorable pressure gradient, for example, one for which (with proper choice of u_∞) $u_1/u_\infty > 1$ and hence $T_1/T_\infty < 1$, an increase of Mach number can be expected to increase λ/C and hence, according to equations (14) and (15), to decrease both Nusselt number and the skin friction. The opposite effect will tend to occur in an adverse pressure gradient.

It should be further noted that for a given ratio G_1 of wall temperature to equilibrium temperature a Mach number effect, independent of the pressure gradient, also appears in the viscosity-temperature factor C according to equations (2) and (13). If $T_0 > S$, then for a fixed G_1 an increase of Mach number M_∞ will diminish C and hence will tend, as far as C is concerned, to diminish both the skin-friction and heat-transfer coefficients in proportion to $\sqrt{C}$. Thus, in a favorable pressure gradient, the dynamical (i.e., T_1/T_∞) and the viscosity (i.e., C) effects of Mach number will tend to amplify each other, while in an adverse pressure gradient they will tend to oppose each other.

It may be worth while to note here that, in view of the fact that λ, and hence δ_t, will ordinarily be only little affected by the wall temperature, equation (3) implies that cooling of the wall will in general tend to diminish the physical boundary-layer thickness. However, for a given value of G_1, the boundary-layer thickness will tend to increase with Mach number.

Numerical Example

In order to illustrate the foregoing general conclusions the boundary layer in the supersonic flow over a thin biconvex circular-arc airfoil of thickness ratio 0.04 (fig. 1) at zero angle of attack was calculated by means of the equations given here.[5] For this case, the

[5] $b_1(\xi)$, however, was calculated by means of equation (68) of reference 2 and not by the approximate equation (10) given here.

velocity distribution outside of the boundary layer can be expressed as (ref. 17)

$$\left.\begin{aligned} u_1/u_\infty &= 1 - k_1\eta - k_2\eta^2 \\ k_1 &= \left(M_\infty^2 - 1\right)^{-1/2} \\ k_2 &= \frac{1}{4\left(M_\infty^2 - 1\right)^2}\left[\gamma M_\infty^4 + \left(M_\infty^2 - 2\right)^2\right] \end{aligned}\right\} \tag{17}$$

where η is the slope of the airfoil at any point along its surface. In equations (17), the subscript ∞ refers specifically to the remote free-stream conditions.

It is in this case convenient, especially for purposes of comparison with flow over a flat plate, to use the point (to be designated by subscript b) immediately behind the shock wave at the leading edge as the reference point.[6] For this purpose, it may be noted that

$$u_1/u_b = \left(u_1/u_\infty\right)/\left(u_b/u_\infty\right)$$

where u_1/u_∞ is given by equations (17), while u_b/u_∞ is obtained from equations (17) by evaluating the slope η at the leading edge. The free-stream Mach number M_∞ can be expressed in terms of the Mach number M_b at point b by means of the relations

$$\left.\begin{aligned} M_b^2 &= M_\infty^2\left(u_b/u_\infty\right)^2\left(T_\infty/T_b\right) \\ T_\infty/T_b &= 1 + \frac{(\gamma - 1)}{2} M_b^2\left(1 - \frac{u_\infty^2}{u_b^2}\right) \end{aligned}\right\} \tag{18}$$

Since in equations (1) to (16) the subscript ∞ refers to any suitable reference point outside of the boundary layer and since in supersonic flow it must refer, in these equations, to a point behind a leading-edge shock wave, it will, for this example, be taken to denote the point b. It will be assumed in this example that $S/T_b = 0.416$.[7] It should be noted that the pressure gradient here is entirely favorable ($u_1' > 0$).

---

[6] In this manner, when comparison is made with flow over a flat plate, the effect of the pressure gradient over the airfoil will be retained, but the effect of the leading-edge shock wave will be essentially eliminated.

[7] In this example, therefore, the temperature T_b outside of the boundary layer immediately behind the leading-edge shock wave, instead of the remote free-stream temperature T_∞, is considered fixed, while the Mach number M_b behind the shock varies.

Figures 2 and 3 show the distribution of local Nusselt number and skin friction for this example, with $M_b = 1.5$ and 3.0 and with $G_1 = 0.3$, 0.5, and 0.7. The results for a flat plate are also shown for comparison. (For $M_b = 1.5$, the value of $\bar{a}_2$ was taken to be $\bar{a}_2 = -1.620G_1$, while, for $M_b = 3.0$, the value $\bar{a}_2 = -1.550G_1$ was used.) Tables I, II, III, and IV give the calculated values of C, λ/C, $b_1/(1 - G_1)$, and a_2, respectively, for the various values of M_b and G_1. In accordance with the general conclusions developed here, it should be expected that, for this example of a favorable pressure gradient, the dynamic effect of wall temperature (i.e., the effect of wall temperature if C were fixed) should be such that lowering the wall temperature diminishes both the Nusselt number and, especially, the skin friction. However, since with the values assumed in this example $T_o/T_b > S/T_b$ in all the cases, the viscosity (or C) effect of wall temperature will here be opposed to the dynamical effect (cf. also tables I and II). Figure 2 indicates that the Nusselt number here increases as the wall temperature is lowered for a given Mach number and hence that the effect of wall temperature arising from the viscosity-temperature relation is the predominant effect here. For the skin friction, however, figure 3 indicates that except near the leading edge ($\xi' < 0.2$) the dynamical effect of the wall temperature is predominant for $M_b = 1.5$, since here C_{f_l} diminishes as the wall is cooled. For $M_b = 3.0$, on the other hand, where T_o/T_b is greater for a given value of G_1 (cf. eq. (13)), so that the C-effect becomes more important than for $M_b = 1.5$, it is seen that the dynamical or pressure-gradient effect of wall temperature predominates only slightly and only after a considerable distance ($\xi' > 0.6$) downstream of the leading edge.

Figure 3 indicates that, for $M_b = 1.5$, lowering the wall temperature brings the skin-friction curves for the airfoil closer to those for a flat plate. This illustrates the general conclusion previously reached regarding the diminution of the direct effect of a pressure gradient by a lowering of the wall temperature. However, for $M_b = 3.0$, figure 3 indicates that the skin-friction curves for the airfoil will now be further removed from those for a flat plate when the wall temperature is lowered. This is essentially due, as previously intimated, to the increased effect, at this higher Mach number, of the temperature distribution $T_1/T_b(\xi)(<1)$ outside of the boundary layer along the airfoil, which tends to increase λ/C and hence diminish C_{f_l} (as well as Nu) in comparison with the value over a flat plate (where $T_1/T_b = 1$). The direct effect of the pressure gradient given by the a_2 term in equation (14), however, is to increase the skin-friction coefficient over that for a flat plate, but at the higher Mach number this effect is not so great as the indirect effect of the pressure gradient due to $T_1/T_b(\xi)$.

The decrease of local Nusselt number for both $M_b = 1.5$ and $M_b = 3.0$ (fig. 2) and the decrease of the local skin-friction coefficient for $M_b = 3.0$ (fig. 3) along the airfoil downstream of the leading edge are due primarily to the decrease, in this region of negative pressure gradient, of the local temperature T_1 outside of the boundary layer (which increases λ/C according to eq. (7)). This, in fact, illustrates the enhanced effect of Mach number on the heat-transfer and skin-friction coefficients due to the pressure gradient.

Table III indicates that the values of b_1 as calculated from equations (67a) and (68) of reference 2 remain fairly close to the value $2(1 - G_1)$ (cf. eq. (10)), although in the present favorable pressure gradient ($a_2 < 0$) they are everywhere less than or equal (at the leading edge) to this value.

LOCATION OF SEPARATION POINT

In a region of adverse pressure gradient (negative u_1') there is a possibility of laminar separation, which occurs where $(\partial u/\partial y)_0 = 0$. A fairly accurate and simple method of calculating the separation point in compressible flows with zero heat transfer was developed in reference 4 and was based in part on the use of an additional boundary condition (first suggested in ref. 3) at the wall necessarily satisfied at the separation point by an exact solution of the partial differential equations. For zero heat transfer, the separation point as a function of Mach number calculated by this method was found to agree very well with numerical solutions in reference 18. (See ref. 4 for details; also, see table V.) In the present section this method will be generalized for any given uniform wall-temperature ratio $G_1 = T_0/T_e$. (For zero heat transfer, as in ref. 4, $G_1 = 1$.)

Method of Calculating Separation Point

By differentiating the momentum partial differential equation of the laminar boundary layer, it can be shown (see the appendix), under the present assumptions of a Prandtl number of 1 and a linear viscosity-temperature relation, that at the separation point

$$\left(\partial^4 u/\partial t^4\right)_0 = 0 \tag{19}$$

with, as well as without, heat transfer at the wall.

A seventh-degree[8] velocity profile in τ can now be chosen to satisfy condition (19) in addition to the boundary conditions satisfied by the sixth-degree profiles (eq. (4)) on which the preceding analysis has been based. From this profile (cf. appendix) it follows that separation will occur where $a_2(\xi)$ has the value (denoted by a_{2s})

$$a_{2s} = \frac{3.5G_1}{G_1 + (2/15)b_1} \tag{20}$$

Moreover, $a_2(\xi)$ is still given by equation (6). From equations (6) and (20) it follows that the value λ_{sep} of λ at the separation point will in general be

$$\lambda_{sep} = -7C \frac{(T_1/T_\infty)^{-(2-\gamma)/(\gamma-1)}}{(u_1'/u_\infty)\left(1 + \frac{\gamma-1}{2} M_1^2\right)} \frac{1}{G_1 + (2/15)b_1} \tag{21}$$

By inserting the approximate equation (10) for b_1 into equation (21),[9] it is found that

$$\lambda_{sep} = -105C \frac{(T_1/T_\infty)^{-(2-\gamma)/(\gamma-1)}}{(u_1'/u_\infty)\left(1 + \frac{\gamma-1}{2} M_1^2\right)} \frac{1}{11G_1 + 4} \tag{22}$$

Moreover, by applying the same type of analysis as described in reference 2 to the seventh-degree velocity profile, the following expression for $\lambda(\xi)$ (denoted by λ_s) can be derived (details are given in the appendix):

$$\lambda_s(\xi) = \frac{7}{2\bar{F}_{1s}} C \frac{\int_0^\xi (u_1/u_\infty)^{\left(2/\bar{F}_{1s}\right)\varphi_{1s}-1} (T_1/T_\infty)^{\left[(2\gamma-1)/(\gamma-1)\right] - \left(\varphi_{1s}/\bar{F}_{1s}\right)} d\xi}{(u_1/u_\infty)^{\left(2/\bar{F}_{1s}\right)\varphi_{1s}} (T_1/T_\infty)^{\left[(\gamma+1)/(\gamma-1) - \left(\varphi_{1s}/\bar{F}_{1s}\right)\right]}} \tag{23}$$

[8]It should be noted that such a seventh-degree velocity profile is used here only for the purpose of determining the separation point and that otherwise the sixth-degree velocity profiles of reference 2 (see also eq. (4)) should be used.

[9]The use of this approximate value greatly simplifies the calculations without appreciably affecting the accuracy. This is due to the fact that equation (10) should ordinarily be a fairly good approximation for b_1 (cf., e.g., table III), while, except in cases of extreme cooling (G_1 close to zero), the b_1 term in equation (20) will be relatively small.

where $\bar{F}_{1s}$ and φ_{1s} are constants given by

$$\left.\begin{aligned}\bar{F}_{1s} &= 0.1159 + 0.002525a_{2s} - 0.001454a_{2s}^2 - 0.0000572(b_1a_{2s}/G_1)^2 - \\ &\quad 0.000574(b_1a_{2s}^2/G_1) + 0.000887(b_1a_{2s}/G_1) \\ \varphi_{1s} &= 0.25G_1 + 0.0437 + 0.0738b_1 + 0.0348a_{2s} - 0.00291a_{2s}^2 + \\ &\quad 0.00773(b_1a_{2s}/G_1) - 0.001147(b_1a_{2s}^2/G_1) - 0.0001145(b_1a_{2s}/G_1)^2\end{aligned}\right\} \quad (24)$$

and b_1 and a_{2s} are simple functions of G_1 according to equations (10) and (20). The constants $\bar{F}_{1s}$ and φ_{1s} are functions of G_1 and are shown in figure 4.

For any given reference Mach number M_∞ and uniform wall-temperature ratio G_1, the separation point in a region of given adverse pressure gradient, as specified by $u_1/u_\infty(\xi)$, will be the station ξ at which the right sides of equations (22) and (23) are equal. Thus, it is necessary, in general, only to plot λ versus ξ, in the anticipated vicinity of separation, in accordance with both equations (22) and (23), and to determine the point of intersection of these two curves. The separation point will evidently be independent of C, so that for the purpose of determining the separation point one may set $C = 1$. In the case of a region of favorable pressure gradient starting at the leading edge followed by a region of unfavorable pressure gradient, equation (23) should be modified to equation (A9) of the appendix, based on the assumption that λ is continuous at the point of discontinuity of the velocity gradient u_1'.

General Implications

With respect to the effect of wall temperature on the separation point, it should be noted, first of all, that, as remarked in the preceding paragraph, the value of the temperature-viscosity factor C has no influence on the separation point. Thus, the temperature-viscosity relation, as it is incorporated in C, does not have the significant effect on the separation point that it has on the skin-friction and heat-transfer coefficients. The effect of wall temperature on the separation point will thus arise only from its dynamical, or pressure-gradient, effect (cf. the section "Skin-Friction and Heat-Transfer Characteristics").

For a fixed velocity distribution $u_1/u_\infty(\xi)$ outside of the boundary layer and a fixed Mach number M_∞, the equations developed here will imply that diminishing the wall temperature, that is, diminishing G_1, will have a favorable effect on separation by moving the separation point downstream. This can be seen particularly from equation (22), according to which the required value of λ for separation (λ_{sep}) will increase as G_1 is diminished. This delay of separation caused by cooling of the wall is an illustration of the general tendency, discussed previously, of a decrease in wall temperature to diminish the direct influence of a pressure gradient (in the present case, an adverse pressure gradient).

The effect of Mach number on the separation point for a fixed value of $u_1/u_\infty(\xi)$ and either a fixed value of G_1 or a fixed value of T_0/T_∞ cannot be predicted quite so readily from the equations as the foregoing effect of wall temperature. Mach number effects are contained in the T_1/T_∞ terms in equations (22) and (23), as well as in the M_1 term of equation (22). These terms tend to cause a decrease in both λ_{sep} and λ_s with increase in Mach number. For a fixed value of G_1, that is, a fixed ratio of actual wall temperature to equilibrium wall temperature for an insulated wall, numerical examples for the case $u_1/u_\infty = 1 - \xi$ have indicated that the effect of Mach number on the required value of λ, that is, λ_{sep} (rather than on λ_s), is the predominant effect, so that under such conditions an increase in Mach number moves the separation point forward and thus enhances separation. A well-known case in this respect is that of zero heat transfer, where $G_1 = 1$ (e.g., refs. 4 and 18). However, according to additional results for the case $u_1/u_\infty = 1 - \xi$, lowering the fixed value of G_1 tends to diminish somewhat this adverse effect of Mach number (ref. 1).

If, instead of considering the ratio G_1 as fixed, the ratio T_0/T_∞ of wall temperature to the reference, or free-stream, temperature is held fixed, then the effect of Mach number on the separation point for a given velocity distribution $u_1/u_\infty(\xi)$ is altered. This is due to the fact that, if T_0/T_∞ is fixed, then, as seen from equation (13), G_1 varies with Mach number, and, in particular, G_1 decreases as M_∞ increases. This effect has a tendency, according to equation (22), to increase the value of λ required for separation as M_∞ is increased. This, in turn, tends to move the separation point downstream, and the numerical example to be subsequently given here indicates that the net effect, at least in the case $u_1/u_\infty = 1 - \xi$, of increasing the Mach number M_∞ as the wall-temperature ratio T_0/T_∞ is fixed is to delay separation. This is hence in contrast with the results obtained for fixed values of G_1, that is, fixed values of T_0/T_e.

Numerical Example

To illustrate quantitatively the application of the equations developed here, as well as the foregoing conclusions, a numerical example based on the case

$$u_1/u_\infty = 1 - \xi \tag{25}$$

will now be given in detail. Equation (25) represents the simplest type of an adverse pressure gradient.[10]

First, the effect of wall temperature on the separation point for a fixed Mach number will be calculated. For this purpose, it will be assumed for simplicity that $M_\infty = 0$ (so that $T_1/T_\infty = 1$) while the parameter G_1 ($G_1 = T_0/T_\infty$ if $M_\infty = 0$) varies. In this case, equating the right sides of equations (22) and (23) leads to the following simple expression for the location of the separation point as a function of the wall temperature ($\xi = \xi_{sep}$):

$$\xi_{sep} = 1 - \left(1 + \frac{60\varphi_{1s}}{11G_1 + 4}\right)^{\left(-\bar{F}_{1s}/2\varphi_{1s}\right)} \tag{26}$$

where φ_{1s} and $\bar{F}_{1s}$ are given in terms of G_1 by equations (24), (10), and (20) or by figure 4. A result qualitatively similar to equation (26) was obtained by the use of fourth-degree profiles in reference 1, but because of the present use of a seventh-degree velocity profile the results based on equation (26) are considerably more accurate quantitatively. The separation point according to equation (26) is plotted in figure 5 for a range of values of T_0/T_∞ from 0.3 to 2.0, and the effect of cooling of the wall in delaying separation can be clearly seen here.

In order to determine the effect of Mach number for a given ratio of wall temperature to free-stream temperature T_0/T_∞, the separation point has been calculated for a range of Mach numbers M_∞ from 0 to 5.31 with a fixed value of T_0/T_∞, namely, $T_0/T_\infty = 2$. The values of G_1, therefore, range from $G_1 = 2$ (for $M_\infty = 0$, wall heated) to $G_1 = 0.3$ (for $M_\infty = 5.31$, wall cooled). The calculations can be performed by observing that by virtue of equations (11) and (12) equation (22) with $\gamma = 1.4$ can be written as

---

[10] If $u_1/u_\infty = 1 - k\xi$, where k is a positive constant, then, as shown in, for example, reference 4, the results based on equation (25) remain valid, with ξ replaced by $k\xi$ and λ replaced by $k\lambda$.

$$\lambda_{sep} = -.105C \frac{(T_1/T_\infty)^{-0.5}}{\left[4 + 11(T_0/T_\infty) + 0.8M_\infty^2\right](u_1'/u_\infty)} \tag{27}$$

Equation (27) is in a form convenient for calculations involving a fixed value of T_0/T_∞. For each specified Mach number M_∞, λ_{sep} as a function of ξ can thus be readily calculated, while $\lambda_s(\xi)$ can be calculated from equations (23) and (24) (or fig. 4) by numerical integration. The value of ξ at which $\lambda_s = \lambda_{sep}$ is then the separation point. The results of such a calculation for the case denoted by equation (25) are shown in figure 6. For comparison, the separation point versus Mach number for zero heat transfer is also included in the figure. The results clearly indicate the favorable effect of Mach number (for the fixed velocity distribution of equation (25)) on the separation point for the fixed value of T_0/T_∞, in contrast with the unfavorable effect of Mach number at zero heat transfer (when G_1 is fixed at unity and hence T_0/T_∞ increases with Mach number: cf. eq. (13)).

Stagnation Flow Followed by Adverse Pressure Gradient

It has already been indicated how the separation point can, in general, be calculated in cases of a favorable pressure gradient followed by an adverse pressure gradient. It may be of interest in this connection to investigate the following question: Under what conditions will the boundary layer in the favorable-gradient region develop to a sufficient extent so that laminar separation will occur almost immediately at the point where the unfavorable gradient starts? In particular, to what extent does the wall temperature affect such conditions? From a practical point of view, this question appears equivalent to the question of when the flow will separate at the point of minimum pressure outside of the boundary layer. It is well known that, at least in incompressible flow without heat transfer, laminar flow usually tends to separate shortly downstream of such a point if the pressure gradient is continuous. In case the favorable pressure gradient can be represented by a stagnation flow, that is, by a flow outside of the boundary layer of the form

$$u_1/u_\infty = K_1\xi \tag{28}$$

where K_1 is a positive constant, and the Mach numbers in this region are sufficiently low so that their effect in this region can be neglected, it will be seen that the foregoing questions can be answered in a particularly simple and fairly interesting manner.

Let the subscript ∞ now denote the point where the adverse pressure gradient starts (here presumed abruptly, that is, discontinuously[11]) after the favorable pressure gradient, and let K_2 be proportional to the magnitude of the negative velocity gradient in the adverse-pressure-gradient region at this point, that is,

$$K_2 = -(u_1'/u_\infty)_{\xi=\xi_{\infty+}} \tag{29}$$

Then, according to equation (22), separation will, in general, occur immediately at this point if λ (denoted here as λ_{fav}) at this point as calculated from the flow in the favorable pressure gradient satisfies the relation[12]

$$\lambda_{fav} \geqq \frac{105}{K_2\left(1 + \frac{\gamma - 1}{2} M_\infty^2\right)} \frac{1}{11G_1 + 4} \tag{30}$$

If, in particular, the region of favorable pressure gradient is a stagnation flow characterized by equation (28), then, applying the results of reference 19 and identifying λ with the quantity κ^2 there,

$$\lambda_{fav} = f(G_1)/K_1 \tag{31}$$

where $f(G_1)$ is a function of G_1 which can be found either from figure 1 of reference 16 or by solving the algebraic equations (30) and (31) there.[13] Substitution for λ_{fav} into relation (30) yields the following condition for immediate separation after the stagnation-flow region:

$$\frac{K_2}{K_1} \geqq \frac{F(G_1)}{1 + \left(\frac{\gamma - 1}{2}\right)M_\infty^2} \tag{32}$$

---

[11]This is, of course, an idealization, since in actuality the pressure gradient will not be discontinuous. However, this idealization might also be regarded as an approximation for a rapidly changing pressure gradient and serves to furnish at least a qualitative answer to the foregoing questions.

[12]It is permitted to put $C = 1$ here since it has already been seen that C does not affect the location of the separation point.

[13] $f(G_1)$ is essentially κ_1^2 for $\varphi = 0$ in reference 19. The quantity h there is equivalent to the quantity G_1 here.

where

$$F(G_1) = \frac{105}{(11G_1 + 4)f(G_1)} \tag{33}$$

In figure 7 $F(G_1)$ is plotted against G_1 for $G_1 = 0$ to 1. As seen from figure 7, $F(G_1)$ varies from 2.40 to 1.00 in this range and increases as G_1 diminishes, that is, as the wall is cooled.

From relation (32) it is seen that the condition, in the present case, for separation at the immediate start of the adverse pressure gradient depends in a simple manner on the magnitude of the ratio of the adverse velocity gradient K_2 to the favorable velocity gradient K_1. Cooling of the wall is seen, once again, to have a tendency to prevent separation, since it increases the minimum required value of K_2/K_1. The Mach number at the beginning of the adverse-pressure-gradient region is, however, seen to have an unfavorable effect.[14]

STABILITY CHARACTERISTICS

It is of interest to investigate the effect of wall temperature, Mach number, and pressure gradient on the stability characteristics of the laminar boundary layer. For this purpose, two types of calculations will be made for the supersonic flow over the thin airfoil (fig. 1) on which the numerical example in the section "Skin-Friction and Heat-Transfer Characteristics" was based. First, the wall temperature required to stabilize the laminar boundary layer completely, that is, for infinite minimum critical Reynolds number, will be calculated at two given stations along the flow for various Mach numbers. Second, the minimum critical Reynolds number at a given station will be calculated as a function of the wall temperature.

The method of calculation is based on the stability criteria developed by Lin and Lees (refs. 5 and 6) with certain modifications presented in an unpublished paper entitled "Calculation of Stability of Constant-Pressure Boundary Layers on Isothermal Surfaces With an Integral-Method Mean-Flow Solution" by Martin Bloom.[15] Explicit details on the method of calculation can also be found in reference 4. The stability criteria as developed by Lin and Lees are based on the amplification or decay of small disturbances, and the minimum critical Reynolds number thereby obtained is the minimum Reynolds number required for the

---

[14]Because of the neglection of Mach number effects in the stagnation-flow region, equations (32) and (33) may not be quantitatively valid for high values of M_∞.

[15]See also references 9 to 11.

possibility that at least certain types (depending on the wave lengths) of disturbances will be amplified. Thus, the existence of a Reynolds number exceeding the minimum critical Reynolds number is a necessary condition for instability of the laminar boundary layer. However, transition to turbulence, which appears to depend on the magnitude of the amplified disturbances, will usually occur at a higher Reynolds number and hence at a point downstream of the point where the actual Reynolds number is equal to the minimum critical Reynolds number. Nevertheless, it can probably be qualitatively concluded that the higher the minimum critical Reynolds number, the more stable the flow and the less the tendency for transition. (Further details on such questions can be found in references 5, 6, and 20.)

Figure 8 shows the wall-temperature ratio T_o/T_b and figure 9, the ratio T_o/T_1 versus the Mach number M_b required for complete stabilization of the flow at two different stations along the airfoil of figure 1. The results for a flat plate (zero pressure gradient) are also included for comparison. Figure 9 clearly indicates, from one viewpoint, the stabilizing influence of the negative pressure gradient here, since the required maximum values of T_o/T_1 for infinite minimum critical Reynolds number are greater for the airfoil than for the flat plate; hence, less cooling, relative to the local temperature T_1 outside of the boundary layer, would be required for the airfoil than for the plate. Figure 9 also indicates that at the higher Mach numbers the stabilizing effect of the favorable pressure gradient appears to be relatively diminished.[16]

These results on the effect of the pressure gradient are qualitatively in accordance with the conclusions of reference 12 (based on zero heat transfer). For the special case of $M_b = 1$, it may be observed, in this connection, that, although infinite cooling ($T_o = 0$) would be required to stabilize the boundary layer over a flat plate completely, only a finite degree of cooling ($T_o > 0$) would suffice to stabilize the flow over the present airfoil. This is due to the fact that the local Mach number increases along the flow over the airfoil, so that when $M_b = 1$ the local Mach number M_1 will exceed unity at the stations along the airfoil downstream of the leading edge.

It is significant to note that the curves for the required maximum values of T_o/T_b (fig. 8) for the airfoil and for the flat plate cross one another at certain Mach numbers M_b. This indicates that, for a fixed reference temperature T_b outside of the boundary layer immediately behind the shock wave at the leading edge, there are Mach

---

[16]This might be due physically, at least in part, to the fact that for the higher Mach numbers M_b the magnitudes of the favorable-velocity-gradient ratio u_1'/u_b according to equations (17) and (18) as well as of the pressure-gradient parameter a_2 (table IV) are decreased.

numbers M_b (for example, $M_b \geqq 2.3$ at $\xi' = 0.8$) for which a lower (uniform) wall temperature would be required on the airfoil than on the flat plate to stabilize the flow completely. This seemingly paradoxical result (in view of the favorable effect of the negative pressure gradient described in the preceding paragraph) is due to the fact that the local temperature T_1 outside of the boundary layer over the airfoil diminishes along the flow and is therefore less than T_b, particularly for the higher Mach numbers (cf. eq. (11), with subscript ∞ replaced by b). Thus, from the viewpoint of complete stabilization, the net effect of the negative pressure gradient at higher Mach numbers is unfavorable with respect to the required temperature ratios T_o/T_b but favorable with respect to the required temperature ratios T_o/T_1, in the sense of figures 8 and 9.

Figure 10 and table VI show the minimum critical Reynolds number $R_{b,cr}$ for the boundary layer at a given station along the airfoil and at two different Mach numbers for both various wall-reference temperature ratios T_o/T_b and various wall-equilibrium temperature ratios G_1. The stabilizing effect of cooling of the wall is clearly indicated here, since the minimum critical Reynolds number is seen to increase as the wall-temperature ratios are diminished. Moreover, by comparison with the results for flow over a flat plate, the stabilizing effect of the negative pressure gradient (by increasing the minimum critical Reynolds number) is also seen in figure 10. The destabilizing influence of a positive pressure gradient is, for zero heat transfer, illustrated by an example in reference 4.

It is interesting to observe the effect of Mach number on the stability of the laminar boundary layer. From figure 10, it is seen that for a fixed ratio G_1 of wall temperature to equilibrium temperature an increase of Mach number from 1.5 to 2.0 destabilizes the boundary layer both over a flat plate and over the airfoil. This effect, for the limited Mach number range considered, is seen, in fact, to be enhanced by the negative pressure gradient here. If, now, instead of a fixed value of G_1, a fixed ratio of wall temperature to reference temperature T_o/T_b is considered, the effect of Mach number, for the limited range under consideration, is changed. For flow without a pressure gradient, an increase of Mach number is now seen from figure 10 to have a stabilizing effect, especially at the lower wall temperatures. For the flow over the airfoil, however, figure 10 (cf. also table VI(a)) now indicates that an increase of Mach number has a stabilizing effect only at wall temperatures close to the critical wall temperature (i.e., for infinite minimum critical Reynolds number) and that for (fixed) higher wall-temperature ratios of T_o/T_b an increase of Mach number has a clear destabilizing effect, similar to the case of fixed values of G_1. Thus, for the low Mach number range treated here, the negative pressure gradient over the airfoil considered here modifies the effect of Mach number on laminar stability for a fixed ratio of wall temperature to reference free-stream temperature.

The critical Reynolds numbers in figure 10 are based on conditions immediately behind the leading-edge shock wave on the airfoil. By comparing these Reynolds numbers with those for a flat plate ($u_1/u_b = 1$), the effect of the actual shock-wave on the stability of the boundary layer is essentially eliminated, so that only the effect of the velocity (or, equivalently, pressure) gradient u_1'/u_b (in addition to the effect of wall temperature) is included here. From a practical viewpoint, it may also be of interest to determine the effect on boundary-layer stability as the flight speed of the supersonic airfoil is increased. For this purpose, the minimum critical free-stream Reynolds number $R_{\infty,cr}$ versus the free-stream Mach number M_∞ has been calculated, and the results are shown in figure 11 and table VI. The results are seen to be quite similar to those based on conditions immediately behind the leading-edge shock wave in the airfoil.

CONCLUSIONS

Under the assumptions of a Prandtl number of 1 and a linear viscosity-temperature relation in conjunction with Sutherland's equation, the following conclusions can be stated from the present investigation of the compressible boundary layer in a pressure gradient over a surface at a given uniform wall temperature. (Interaction between the boundary layer and the external stream has not been considered.)

1. The effect of wall temperature on the skin-friction and heat-transfer coefficients arises from the pressure gradient and (independently of the pressure gradient) from the factor C in the viscosity-temperature relation. ($C = (T_0/T_\infty)^{1/2}(T_\infty + S)/(T_0 + S)$ where T_0 is the temperature at the wall, T_∞ is the temperature at a point outside the boundary layer, and S is the Sutherland constant.) In regard to the pressure-gradient effect, cooling of the wall tends to diminish the Nusselt number and, especially, the skin friction in a favorable (negative) pressure gradient and to increase the coefficients in an adverse (positive) pressure gradient. In regard to the temperature-viscosity effect, lowering the wall-temperature ratio T_0/T_∞ will ordinarily tend to increase both the skin friction and Nusselt number.

2. Cooling of the wall tends, in general, to diminish the direct effect of a pressure gradient. A particularly clear example of this is the delay of separation in an adverse pressure gradient by cooling of the wall.

3. A simple and ordinarily sufficiently accurate method of determining the separation point in a given subsonic or supersonic adverse

pressure gradient over a wall at any specified uniform wall temperature has been developed here.

4. The results of a numerical example for a fixed linearly decreasing velocity outside of the boundary layer indicate, in addition to the delaying of separation by cooling of the wall, that, for a fixed ratio G_1 of wall temperature to equilibrium adiabatic wall temperature, an increase of free-stream Mach number moves the separation point upstream; while, for a fixed ratio T_O/T_∞ of wall temperature to free-stream temperature, an increase of Mach number has, in general, a less unfavorable effect and in this case actually moves the separation point downstream.

5. Numerical examples for the supersonic flow over a thin airfoil indicate in detail the stabilizing nature of a negative pressure gradient and of cooling of the wall on the laminar boundary layer. The examples also indicate that the pressure gradient here modifies the effect of Mach number on laminar stability for a fixed ratio of wall temperature to reference free-stream temperature.

Polytechnic Institute of Brooklyn,
Brooklyn, N. Y., April 7, 1954.

APPENDIX

DETERMINATION OF SEPARATION POINT

When the assumptions that the Prandtl number is 1 and that the coefficient of viscosity is proportional to the absolute temperature (eq. (1)) are made, differentiation of the momentum partial differential equation with respect to t yields the following relation at the wall (cf. eq. (25) of ref. 2), where $u = v = 0$:

$$\left(\frac{\partial^3 u}{\partial t^3}\right)_o = \frac{1}{T_o}\left(\frac{\partial T}{\partial t}\frac{\partial^2 u}{\partial t^2}\right)_o \tag{A1}$$

Moreover, the energy partial differential equation and differentiation of this equation with respect to t yield the following relations for a uniform wall temperature (cf. eqs. (26) and (27) of ref. 2):

$$\left.\begin{aligned}\left(\partial^2 H/\partial t^2\right)_o &= 0\\ \left(\partial^3 H/\partial t^3\right)_o &= 0\end{aligned}\right\} \tag{A2}$$

where

$$H \equiv \left(u^2/2\right) + c_p T \tag{A3}$$

From equations (A2) and (A3) it follows that at the separation point, that is, where

$$\left(\partial u/\partial t\right)_o = 0 \tag{A4}$$

the relation

$$\left(\partial^2 T/\partial t^2\right)_o = 0 \tag{A5}$$

holds. Differentiating the momentum partial differential equation twice with respect to t and taking values at the separation point, it is found, with the use of equations (A1) to (A5), that

$$\left(\partial^4 u/\partial t^4\right)_o = 0 \tag{A6}$$

which is in accord with equation (19) of the main text.

The seventh-degree velocity profile in τ satisfying condition (A6) in addition to the boundary conditions (viz., eqs. (22) to (28) of ref. 2) satisfied in the present analysis by the sixth-degree profiles is

$$\frac{u}{u_1} = \left(\frac{7}{4}\tau - \frac{21}{4}\tau^5 + 7\tau^6 - \frac{5}{2}\tau^7\right) + a_2\left(-\frac{1}{2}\tau + \tau^2 - \frac{5}{2}\tau^5 + 3\tau^6 - \tau^7\right) + a_3\left(-\frac{1}{5}\tau + \tau^3 - 3\tau^5 + \frac{16}{5}\tau^6 - \tau^7\right) \tag{A7}$$

where a_2 is given by equation (6), while

$$a_3 = \left(a_2 b_1\right)/\left(3G_1\right) \tag{A8}$$

The condition $(\partial u/\partial t)_0 = 0$ will, according to equations (A7) and (A8), lead to equation (20) of the main text.

By inserting the profile (A7), in conjunction with equation (A8), into the momentum integral-differential equation (11) of reference 2 and assuming, as in reference 2, that the a_2 and b_1 terms in F_1 and F_2 (defined in ref. 2) may be replaced by constant values, an ordinary differential equation of the same form as equation (9) of the main text is obtained, except that $\bar{F}_1$ and φ_1 (now written as $\bar{F}_{1s}$ and φ_{1s}) are now given by equations (24) of the main text, while the factor 2 on the right side of equation (9) is replaced by 7/4. Comparison, accordingly, with the solution of equation (9) (eq. (7)), leads to equation (23) of the main text. Since the chief purpose is here the location of the separation point, the constant value of a_2 (as in ref. 4) is now chosen as that at the separation point and hence as that given by equation (20) of the main text.

In case the region of adverse pressure gradient starts at some point $\xi = \xi_a$ downstream of the leading edge, then equation (23) can still be applied directly in calculating the separation point. Greater accuracy, however, might be obtained in such a case by applying equation (23) only for the region of adverse pressure gradient. For this purpose, equation (23) must be modified to satisfy the boundary condition $\lambda = \lambda_a$ at $\xi = \xi_a$. Thus,

$$\lambda_s = \frac{(I)_{\xi=\xi_a}\,\lambda_a + \frac{7}{2}\,C\int_{\xi_a}^{\xi}(u_1/u_\infty)^{\frac{2}{\bar{F}_{1s}}\varphi_{1s}-1}\,(T_1/T_\infty)^{\frac{2\gamma-1}{\gamma-1}-\frac{\varphi_{1s}}{\bar{F}_{1s}}}\,d\xi}{I} \tag{A9}$$

where

$$I = (u_1/u_\infty)^{\frac{2}{\bar{F}_{1s}}\varphi_{1s}} (T_1/T_\infty)^{\frac{\gamma+1}{\gamma-1}-\frac{\varphi_{1s}}{\bar{F}_{1s}}}$$

and where λ_a can be obtained as the value of λ at $\xi = \xi_a$ based on equation (7) for the region $\left(0 \leqq \xi < \xi_a\right)$ of favorable pressure gradient.

REFERENCES

1. Morduchow, Morris, and Galowin, Lawrence: The Compressible Laminar Boundary Layer in a Pressure Gradient Over a Surface Cooled by Fluid Injection. Proc. First Iowa Thermodynamics Symposium, State Univ. of Iowa, Apr. 27-28, 1953.

2. Libby, Paul A., and Morduchow, Morris: Method for Calculation of Compressible Laminar Boundary Layer With Axial Pressure Gradient and Heat Transfer. NACA TN 3157, 1954.

3. Timman, R.: A One Parameter Method for the Calculation of Laminar Boundary Layers. Rep. F. 35, Nationaal Luchtvaartlaboratorium, 1949, pp. F29-F46.

4. Morduchow, Morris, and Clarke, Joseph H.: Method for Calculation of Compressible Laminar Boundary-Layer Characteristics in Axial Pressure Gradient With Zero Heat Transfer. NACA TN 2784, 1952.

5. Lin, Chia Chiao, and Lees, Lester: Investigation of the Stability of the Laminar Boundary Layer in a Compressible Fluid. NACA TN 1115, 1946.

6. Lees, Lester: The Stability of the Laminar Boundary Layer in a Compressible Fluid. NACA Rep. 876, 1947. (Supersedes NACA TN 1360.)

7. Lin, C. C.: On the Stability of the Boundary Layer With Respect to Disturbances of Large Wave Velocity. Readers' Forum, Jour. Aero. Sci., vol. 19, no. 2, Feb. 1952, pp. 138-139.

8. Van Driest, E. R.: Calculation of the Stability of the Laminar Boundary Layer in a Compressible Fluid on a Flat Plate With Heat Transfer. Jour. Aero. Sci., vol. 19, no. 12, Dec. 1952, pp. 801-812, 828.

9. Bloom, Martin: The Effect of Surface Cooling on Laminar Boundary-Layer Stability. Readers' Forum, Jour. Aero. Sci., vol. 18, no. 9, Sept. 1951, pp. 635-636.

10. Bloom, Martin: Further Comments on "The Effect of Surface Cooling in Laminar Boundary-Layer Stability." Readers' Forum, Jour. Aero. Sci., vol. 19, no. 5, May 1952, p. 359.

11. Bloom, Martin: On the Calculation of Laminar Boundary-Layer Stability. Readers' Forum, Jour. Aero. Sci., vol. 21, no. 3, Mar. 1954, pp. 207-210.

12. Weil, Herschel: Effects of Pressure Gradient on Stability and Skin Friction in Laminar Boundary Layers in Compressible Fluids. Jour. Aero. Sci., vol. 18, no. 5, May 1951, pp. 311-318.

13. Chapman, D. R., and Rubesin, M. W.: Temperature and Velocity Profiles in the Compressible Laminar Boundary Layer With Arbitrary Distribution of Surface Temperature. Jour. Aero. Sci., vol. 16, no. 9, Sept. 1949, pp. 547-565.

14. Fluid Motion Panel of the Aeronautical Research Committee and Others (S. Goldstein, ed.): Modern Developments in Fluid Dynamics. Vol. II. The Clarendon Press (Oxford), 1938, pp. 623-627, 631-632.

15. Levy, Solomon: Heat Transfer to Constant-Property Laminar Boundary-Layer Flows With Power-Function Free-Stream Velocity and Wall-Temperature Variation. Jour. Aero. Sci., vol. 19, no. 5, May 1952, pp. 341-348.

16. Low, George M.: The Compressible Laminar Boundary Layer With Heat Transfer and Small Pressure Gradient. NACA TN 3028, 1953.

17. Ferri, Antonio: Elements of Aerodynamics of Supersonic Flows. The Macmillan Co., 1949, pp. 125-127.

18. Stewartson, K.: Correlated Incompressible and Compressible Boundary Layers. Proc. Roy. Soc. (London), ser. A, vol. 200, no. 1060, Dec. 22, 1949, pp. 84-100.

19. Morduchow, Morris: On Heat Transfer Over a Sweat-Cooled Surface in Laminar Compressible Flow With a Pressure Gradient. Jour. Aero. Sci., vol. 19, no. 10, Oct. 1952, pp. 705-712.

20. Lees, Lester: Instability of Laminar Flows and Transition to Turbulence. Rep. ZA-7-006, Consolidated Vultee Aircraft Corp., Feb. 25, 1952.

TABLE I

VALUES OF TEMPERATURE-VISCOSITY FACTOR C

VERSUS

MACH NUMBER AND WALL-TEMPERATURE RATIO

M_b	1.5			3.0.		
G_1	0.3	0.5	0.7	0.3	0.5	0.7
C	1.097	1.057	0.997	1.033	0.923	0.834

TABLE II

VALUES OF λ/C ALONG AIRFOIL OF FIGURE 1

ξ'	λ/C at M_b of -					
	1.5			3.0		
	$G_1 = 0.3$	$G_1 = 0.5$	$G_1 = 0.7$	$G_1 = 0.3$	$G_1 = 0.5$	$G_1 = 0.7$
0	0	0	0	0	0	0
.1	3.73	3.74	3.76	3.92	3.94	3.95
.2	7.49	7.49	7.51	8.27	8.28	8.28
.3	11.32	11.28	11.26	13.07	13.03	13.01
.4	15.22	15.11	15.02	18.34	18.24	18.14
.5	19.23	19.01	18.83	24.12	23.91	23.70
.6	23.35	23.01	22.72	30.41	30.08	29.71
.7	27.56	27.09	26.67	37.29	36.73	36.18
.8	31.86	31.22	30.67	44.50	43.70	43.00
.9	36.41	35.56	34.82	52.30	51.29	50.32
1.0	41.01	39.95	39.01	60.49	59.18	57.90

TABLE III

VALUES OF $b_1/(1 - G_1)$ ALONG AIRFOIL OF FIGURE 1

ξ'	$b_1/(1 - G_1)$ at M_b of -					
	1.5			3.0		
	$G_1 = 0.3$	$G_1 = 0.5$	$G_1 = 0.7$	$G_1 = 0.3$	$G_1 = 0.5$	$G_1 = 0.7$
0	2.000	2.000	2.000	2.000	2.000	2.000
.1	1.978	1.975	1.969	1.980	1.976	1.974
.2	1.959	1.953	1.945	1.963	1.958	1.949
.3	1.944	1.935	1.927	1.947	1.939	1.929
.4	1.932	1.921	1.910	1.935	1.924	1.913
.5	1.923	1.910	1.897	1.924	1.913	1.900
.6	1.914	1.901	1.889	1.916	1.904	1.900
.7	1.908	1.895	1.882	1.910	1.898	1.883
.8	1.904	1.890	1.879	1.905	1.894	1.879
.9	1.901	1.887	1.877	1.902	1.891	1.879
1.0	1.898	1.886	1.876	1.900	1.890	1.876

TABLE IV

VALUES OF $-a_2$ ALONG AIRFOIL OF FIGURE 1

ξ'	$-a_2$ at M_b of -					
	1.5			3.0		
	$G_1 = 0.3$	$G_1 = 0.5$	$G_1 = 0.7$	$G_1 = 0.3$	$G_1 = 0.5$	$G_1 = 0.7$
0	0	0	0	0	0	0
.1	.1205	.2017	.2840	.1077	.1802	.2536
.2	.2315	.3859	.5414	.2128	.3548	.4972
.3	.3351	.5567	.7777	.3141	.5219	.7296
.4	.4309	.7130	.9920	.4113	.6816	.9492
.5	.5202	.8574	1.1890	.5029	.8306	1.1527
.6	.6044	.9928	1.3721	.5881	.9696	1.3408
.7	.6798	1.1140	1.5355	.6669	1.0949	1.5098
.8	.7513	1.2271	1.6877	.7331	1.2002	1.6531
.9	.8175	1.3305	1.8239	.7899	1.2911	1.7730
1.0	.8764	1.4231	1.9454	.8391	1.3565	1.8579

TABLE V

SEPARATION POINT CALCULATED AS A FUNCTION OF MACH NUMBER FOR ZERO HEAT TRANSFER ($G_1 = 1$) AND $u_1/u_\infty = 1 - \xi$

	ξ_{sep} for M_∞ of -			
	0	1	3	10
Based on eqs. (22) to (24)	0.122	0.113	0.0768	0.023
Based on method of Stewartson (ref. 15)	0.120	0.110	0.077	0.024

TABLE VI

MINIMUM CRITICAL REYNOLDS NUMBERS OF LAMINAR BOUNDARY LAYER OVER AIRFOIL IN FIGURE 1 AND OVER A FLAT PLATE

(a) Over airfoil ($\xi' = 0.8$)

M_b	M_∞	G_1	T_o/T_b	T_o/T_∞	$R_{b,cr}$	$R_{\infty,cr}$
1.5	1.662	1.1	1.595	1.708	2.69×10^4	2.59×10^4
		1.0	1.450	1.553	6.58	6.34
		.93	1.348	1.443	48.6	46.86
		.91	1.320	1.413	128.6	124.0
		.90	1.305	1.397	261.3	251.9
		.888	1.288	1.379	∞	∞
2.0	2.184	1.0	1.8	1.94	0.217	0.201
		.9	1.62	1.74	.389	.362
		.8	1.44	1.55	1.777	1.653
		.77	1.386	1.49	4.448	4.137
		.737	1.327	1.43	∞	∞

(b) Over flat plate

$M_b = M_\infty$	G_1	T_o/T_b	T_o/T_∞	$R_{b,cr}$	$R_{\infty,cr}$
1.5	1.2	1.740	1.740	0.0804×10^4	0.0804×10^4
	1.0	1.450	1.450	.282	.282
	.95	1.378	1.378	.426	.426
	.90	1.305	1.305	.641	.641
	.75	1.088	1.088	16.68	16.68
	.72	1.044	1.044	322.2	322.2
	.7166	1.039	1.039	∞	∞
2.0	1.00	1.8	1.8	0.0506	0.0506
	.90	1.62	1.62	.0903	.0903
	.75	1.35	1.35	.481	.481
	.70	1.26	1.26	1.648	1.648
	.683	1.229	1.229	∞	∞

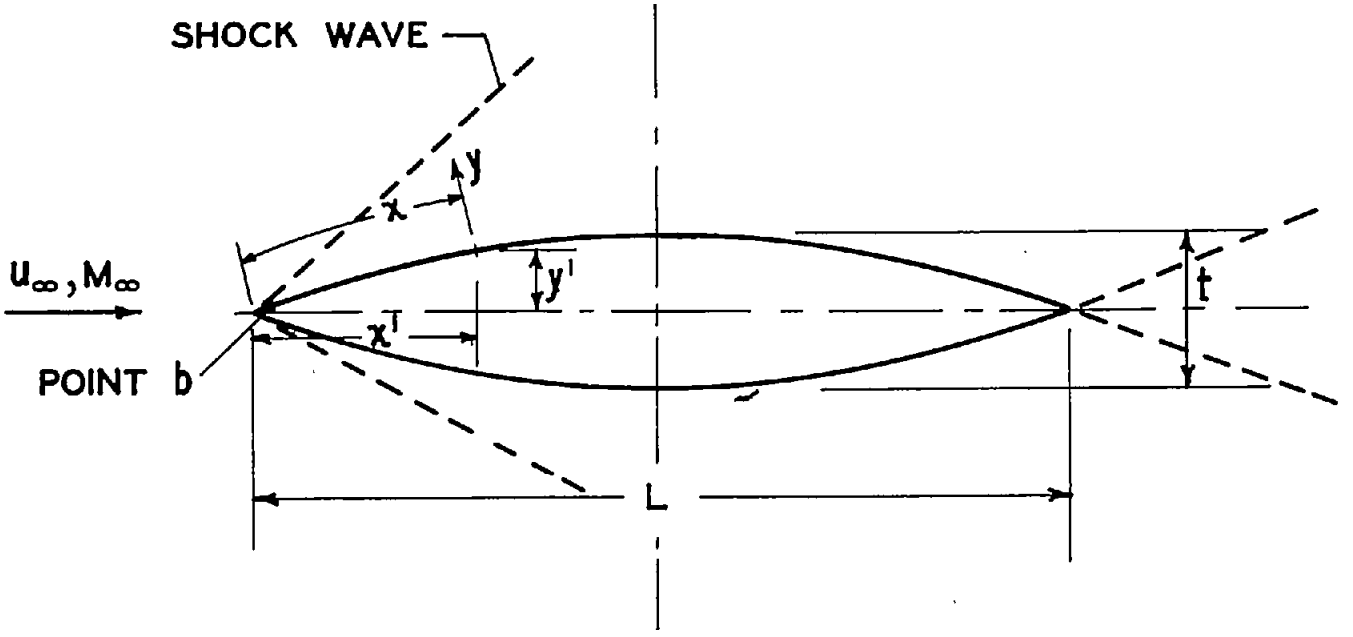

Figure 1.- Thin circular-arc biconvex airfoil in supersonic flow. $t/L = 0.04$, $\eta \equiv dy'/dx'$, and $\xi' \equiv x'/L$.

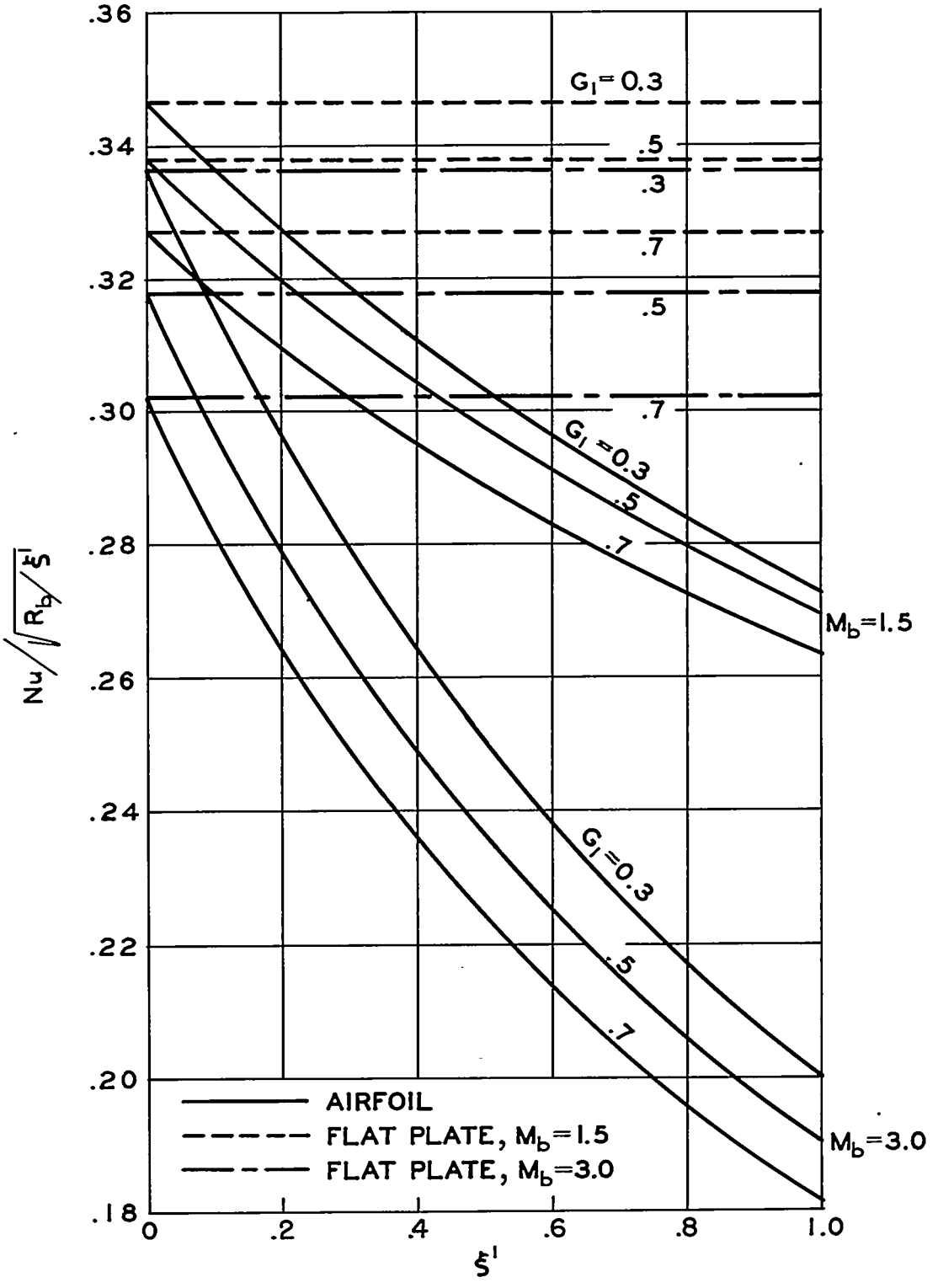

Figure 2.- Distribution of local Nusselt number along thin supersonic airfoil and along flat plate.

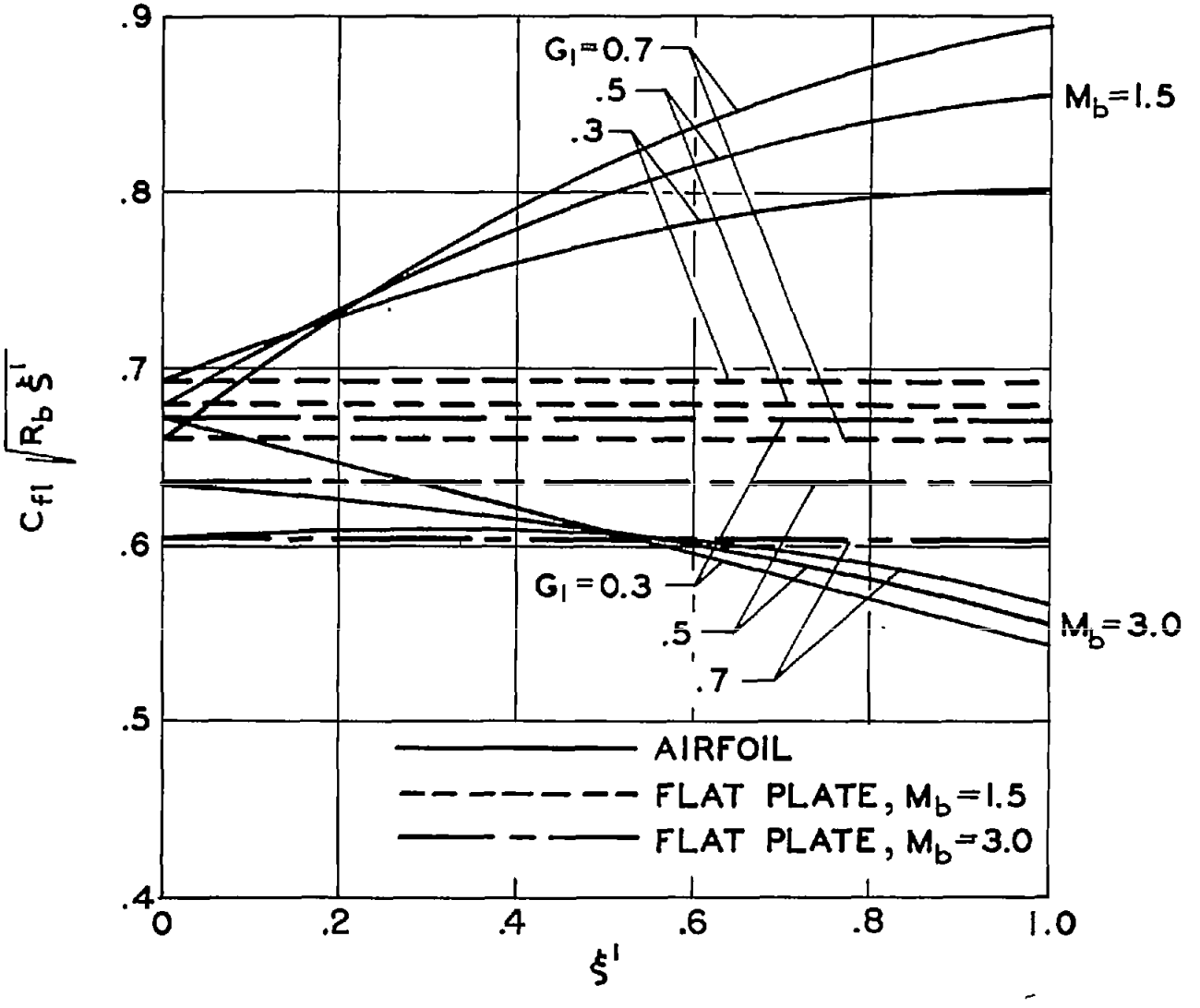

Figure 3.- Distribution of local skin-friction coefficient along thin supersonic airfoil and along flat plate.

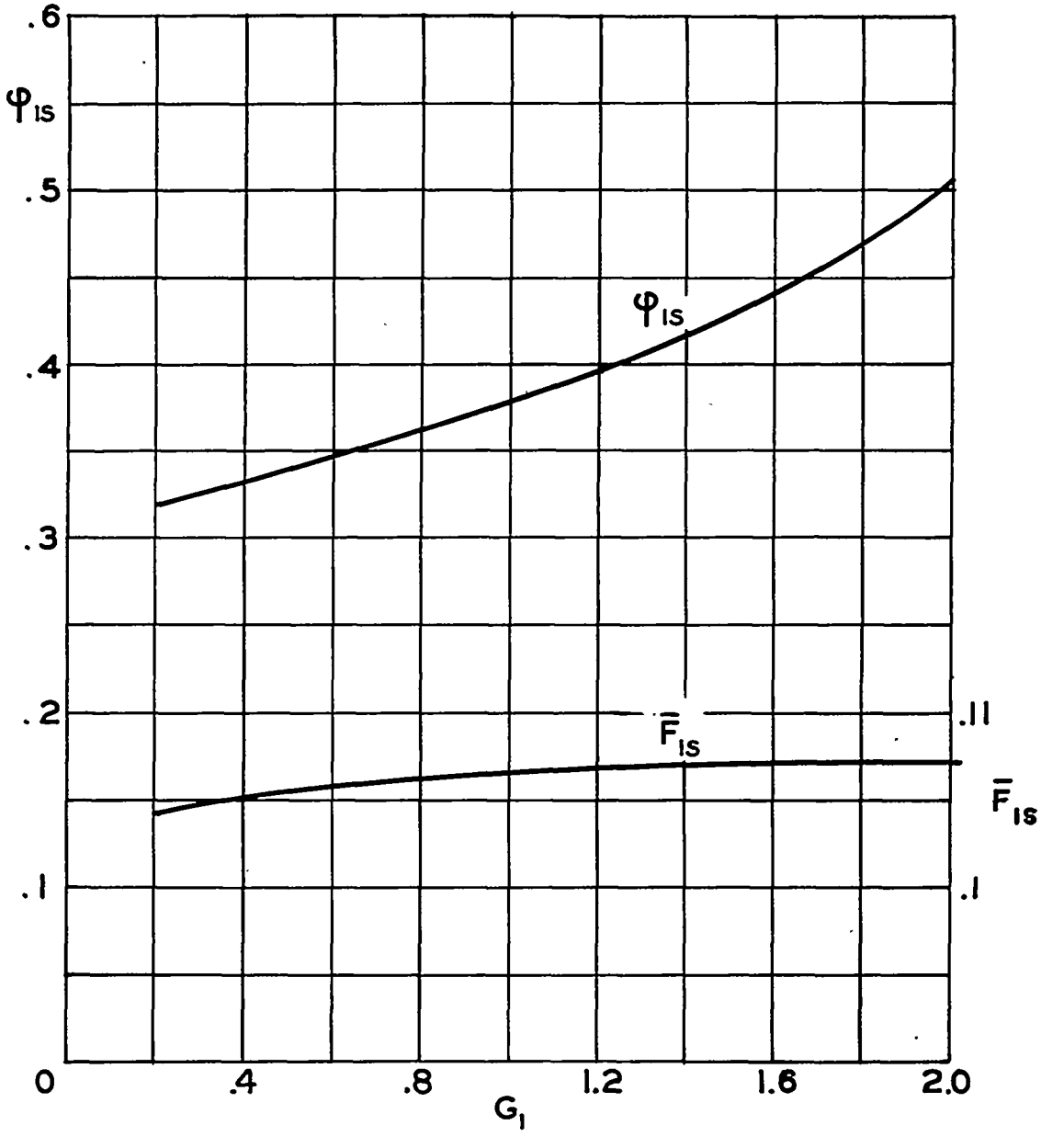

Figure 4.- $\bar{F}_{1s}$ and φ_{1s} as functions of G_1.

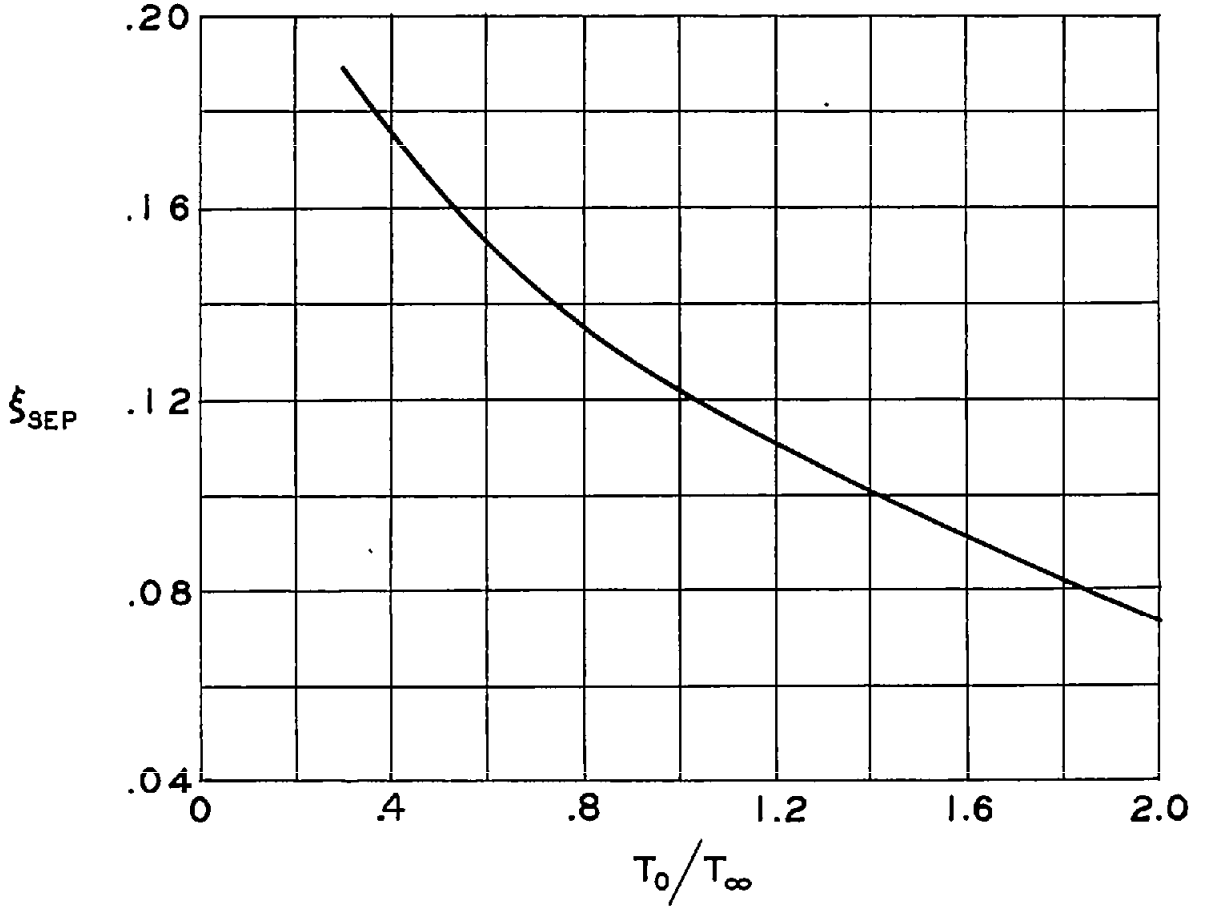

Figure 5.- Separation point as a function of wall temperature (incompressible flow). $\frac{u_1}{u_\infty} = 1 - \xi$ and $M_\infty = 0$.

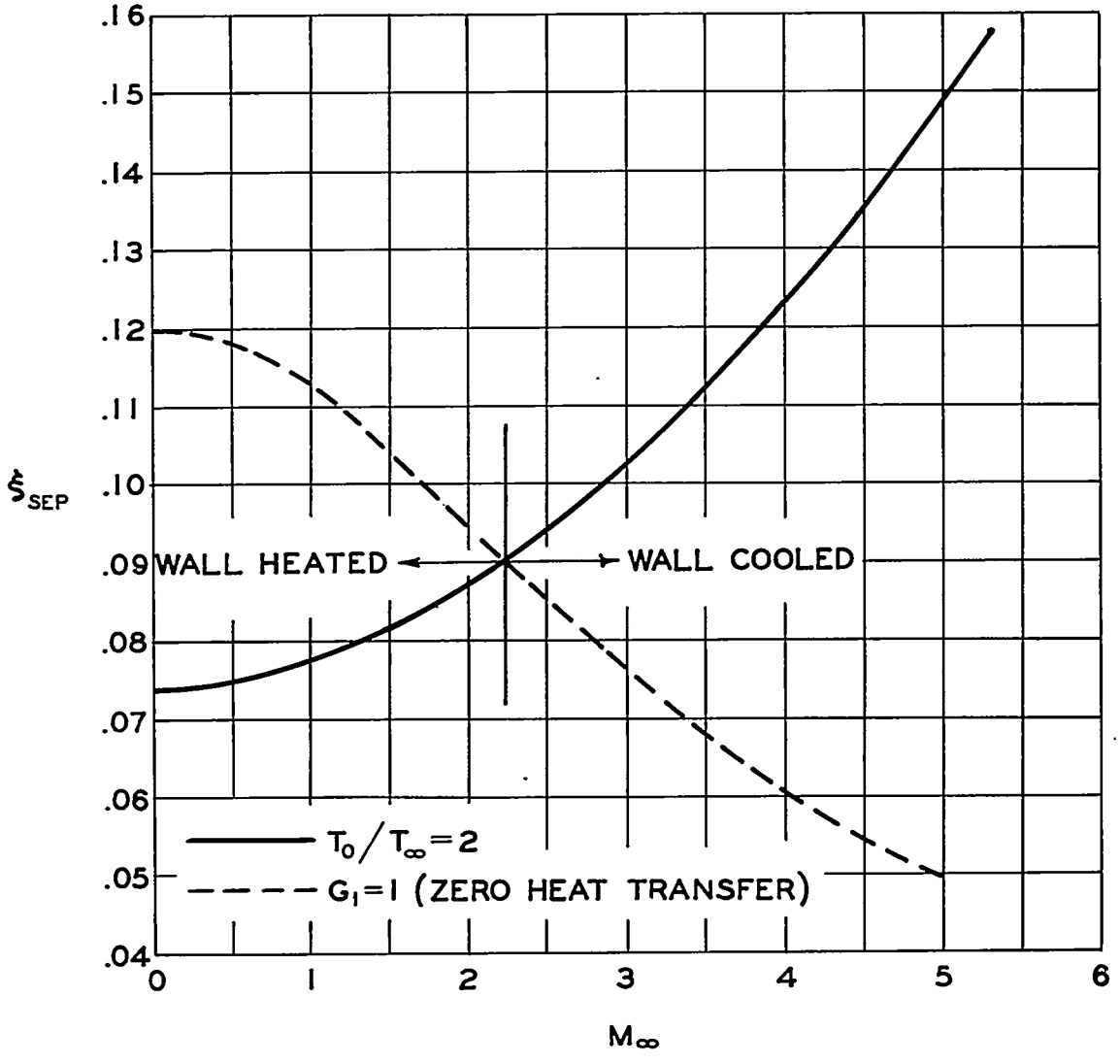

Figure 6.- Separation point as a function of Mach number. $\frac{u_1}{u_\infty} = 1 - \xi$.

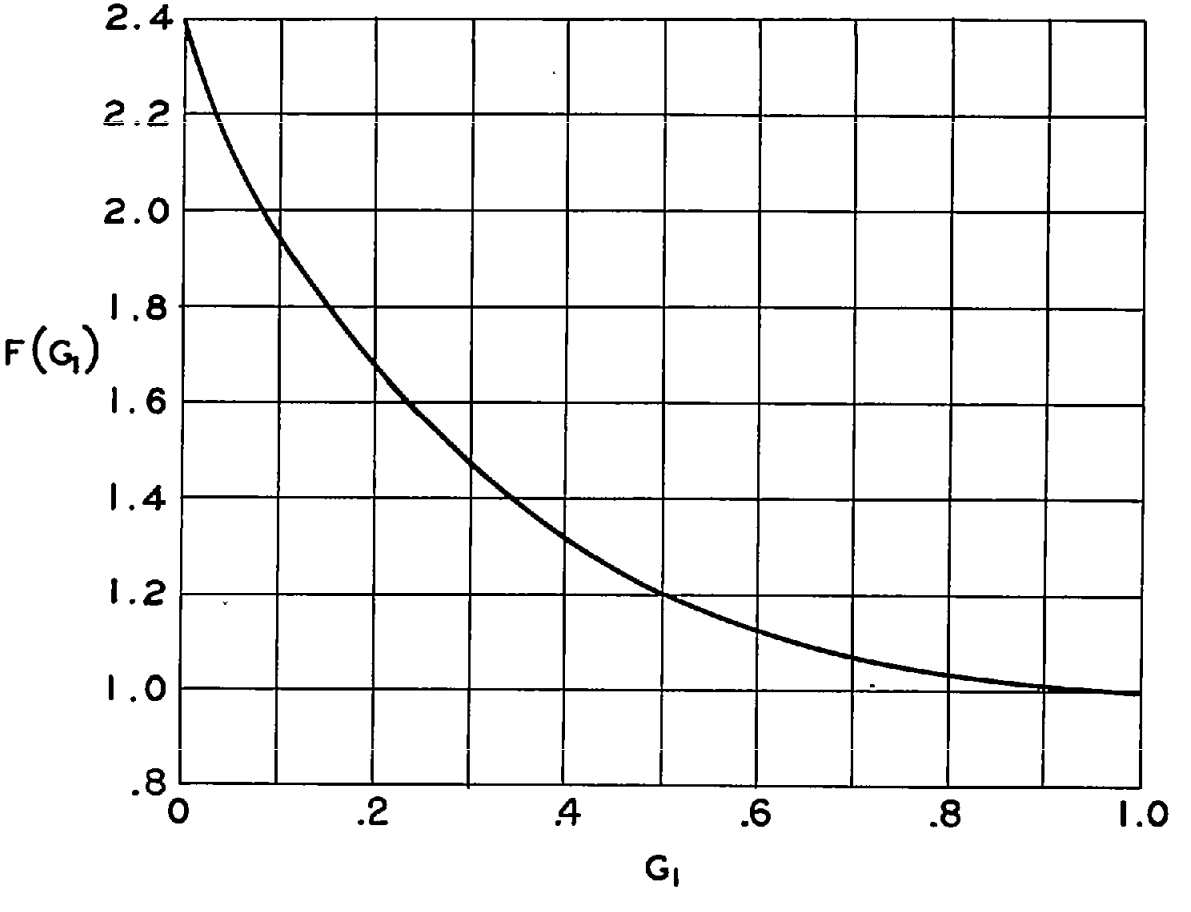

Figure 7.- $F(G_1)$ in condition (32).

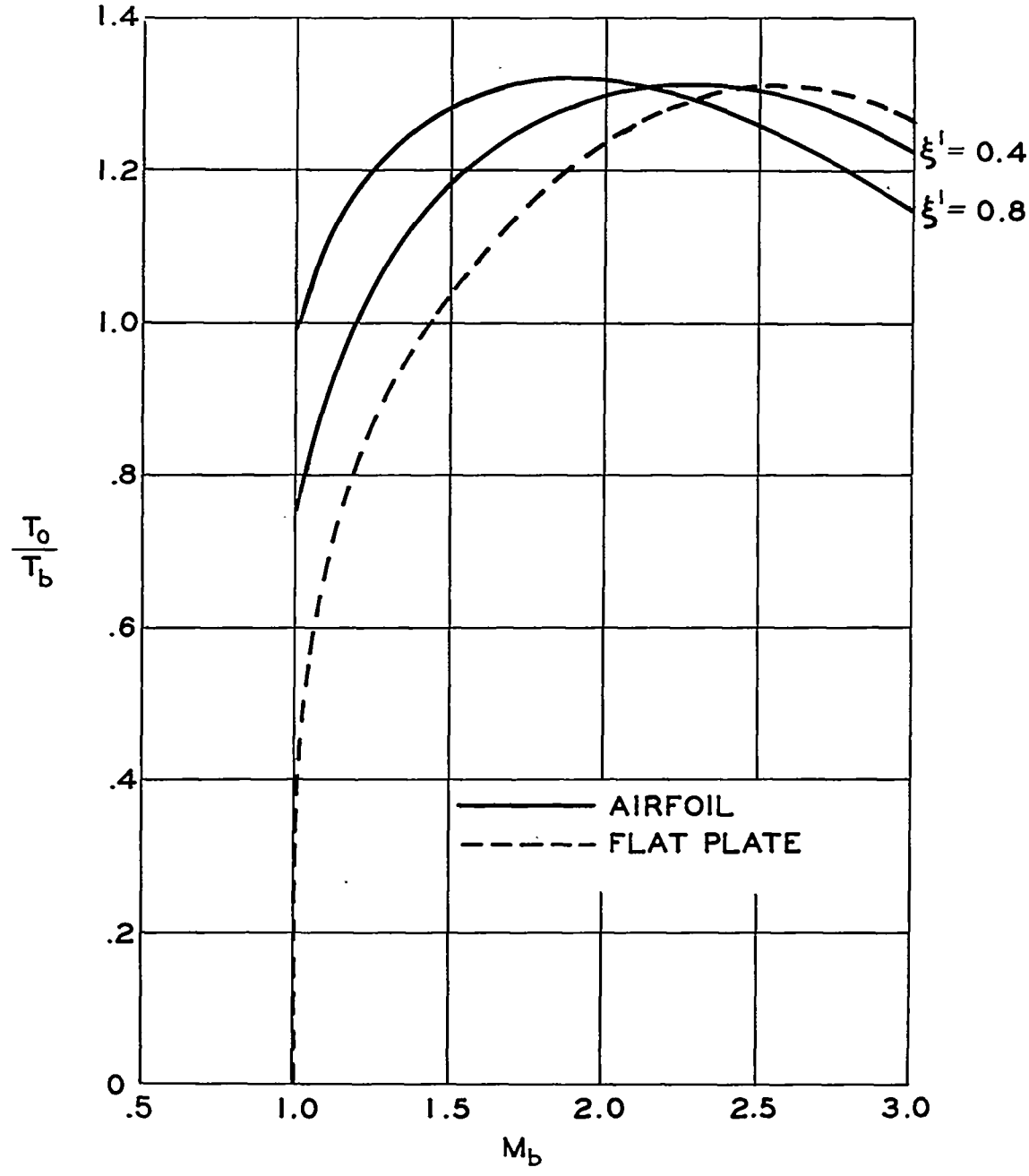

Figure 8.- Wall-reference-temperature ratios T_o/T_b required for infinite minimum critical Reynolds number.

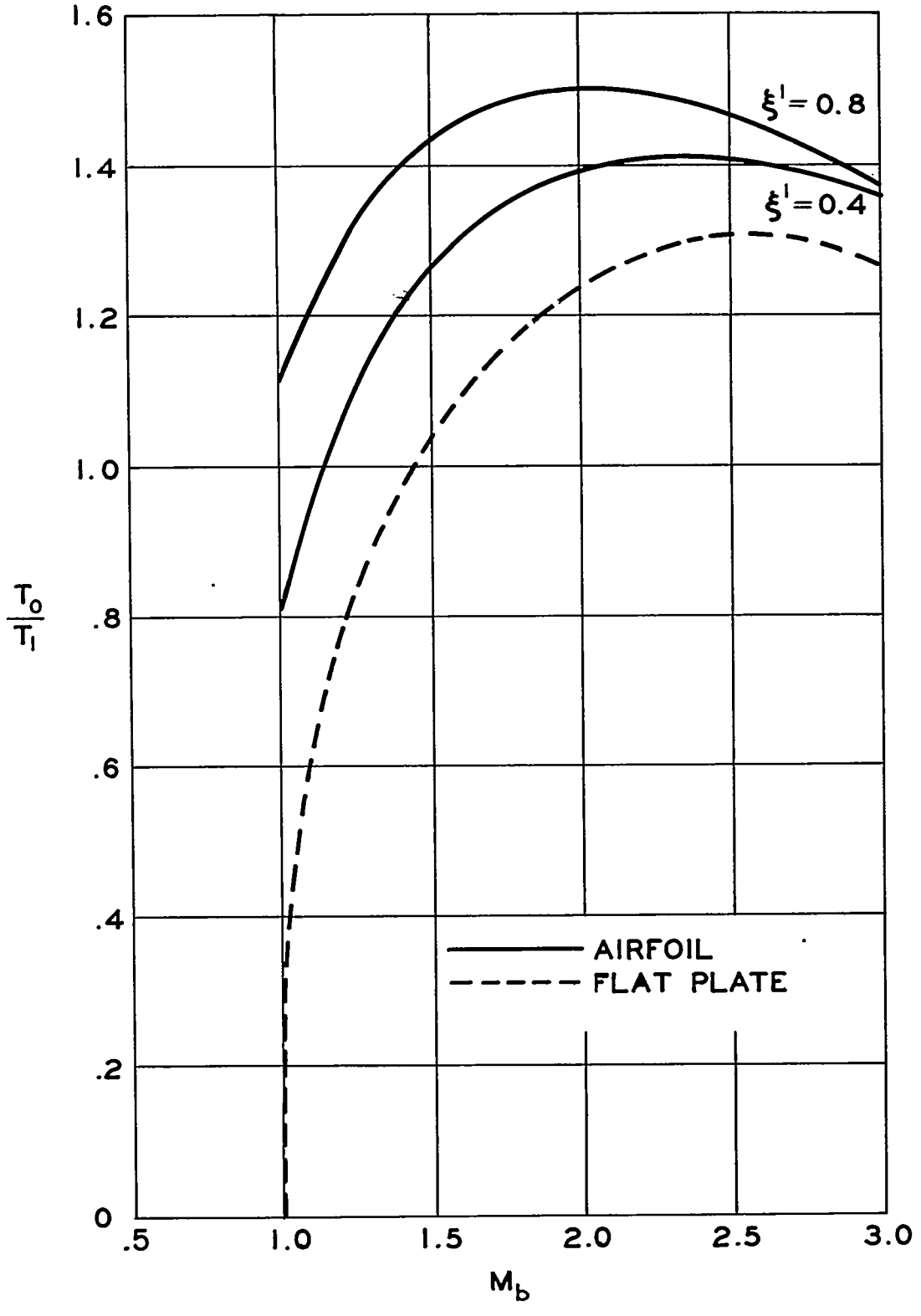

Figure 9.- Ratios of wall to local main-stream wall temperature T_o/T_1 required for infinite minimum critical Reynolds number.

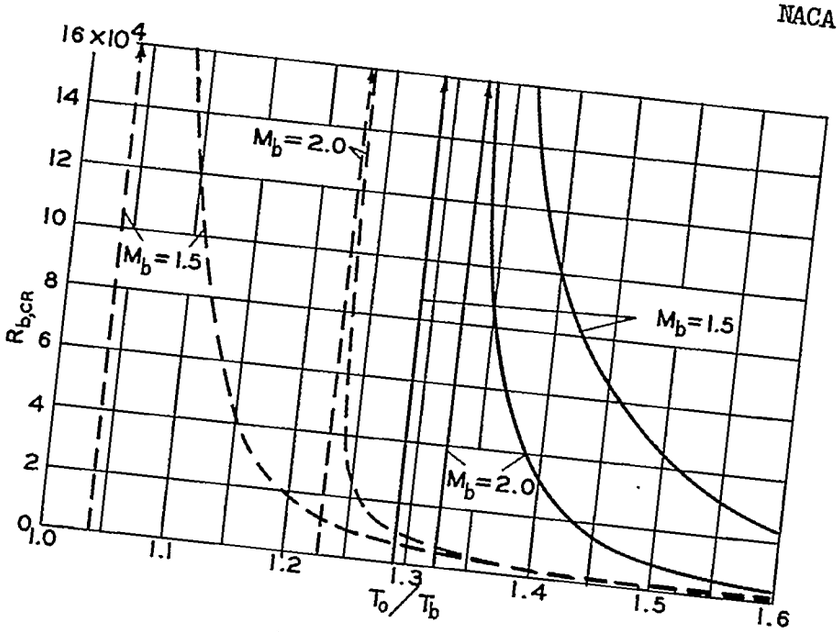

(a) $R_{b,cr}$ against T_o/T_b.

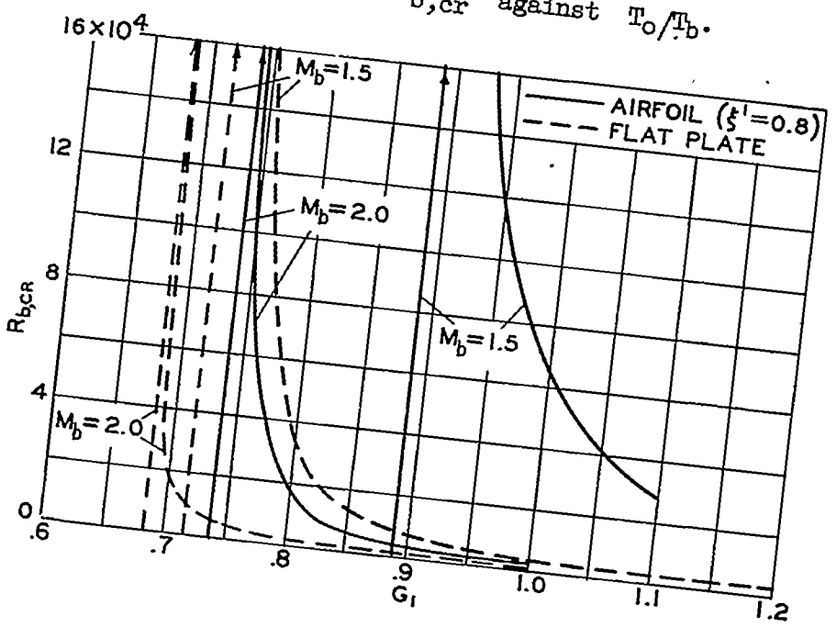

(b) $R_{b,cr}$ against G_1.

Figure 10.- Minimum critical Reynolds numbers $R_{b,cr}$ versus Mach number M_b, wall-reference-temperature ratio T_o/T_b, and wall-equilibrium-temperature ratio G_1. Vertical lines with arrows indicate corresponding asymptotes; compare table VI.

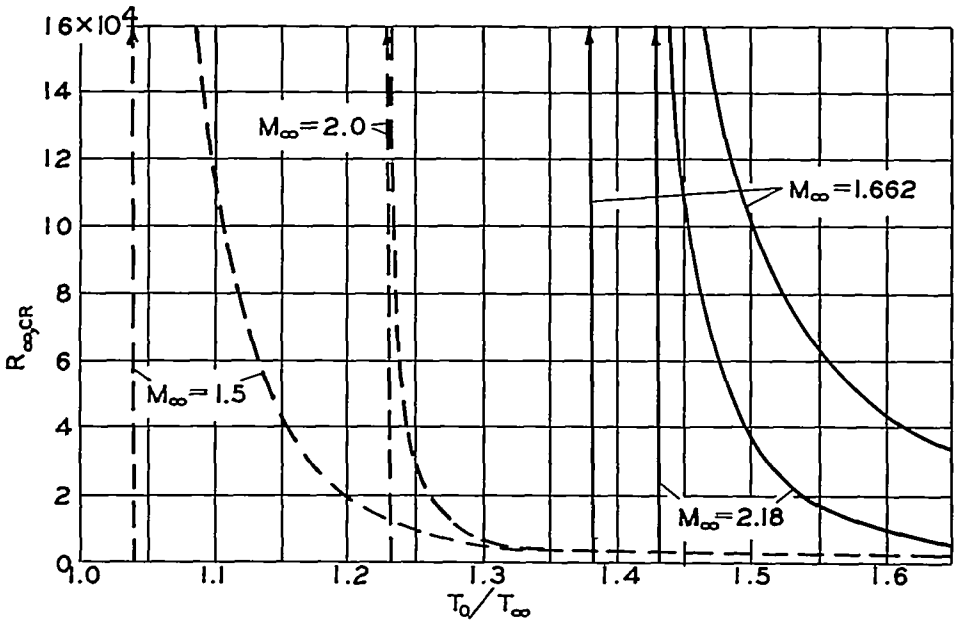

(a) $R_{\infty,cr}$ against T_0/T_∞.

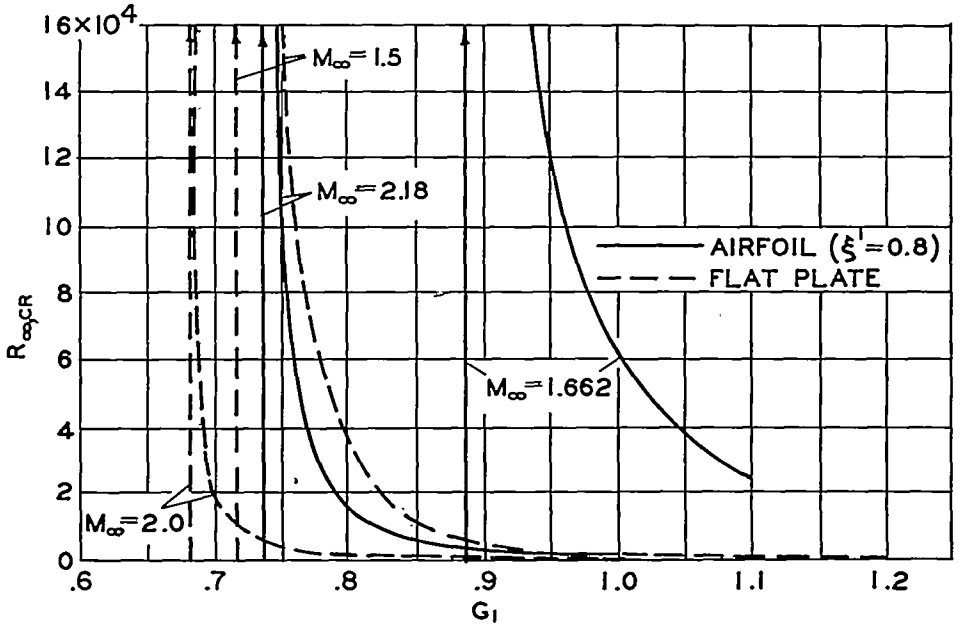

(b) $R_{\infty,cr}$ against G_1.

Figure 11.- Minimum critical Reynolds numbers $R_{\infty,cr}$ versus Mach number M_∞, wall-reference-temperature ratio T_0/T_∞, and wall-equilibrium-temperature ratio G_1. Vertical lines with arrows indicate corresponding asymptotes; compare table VI.